Utrecht University

Institute for Theoretical Physics

Master's Thesis

Inflaton Perturbations from Slow-Roll inflation to Ultra-Slow-Roll inflation

Author:
Lotte Spanjers, BSc

Supervisor:
Dr. Tomislav Prokopec

July 12, 2019

Universiteit Utrecht

Abstract

Recently, in the search for the nature of dark matter, interest in alternatives to the WIMP-paradigm has been renewed. One such an alternative is the idea that dark matter consists of primordial black holes (PBHs), which were created by the gravitational collapse of over-dense regions in the early universe. It was recently realized that a previously unrecognised regime of inflation exists, in which the slow-roll (SR) approximation breaks down, giving rise to the so-called ultra-slow-roll (USR) regime. During this regime, the primordial power spectrum can experience rapid growth, and therefore give rise to more PBHs. In this thesis, we match a period of USR inflation to a period of SR inflation, and analyse the growth of the curvature perturbations. We do this with taking corrections of order ϵ, which are often neglected, into account. We also make sure the background (the scale factor and Hubble parameter) is smoothly matched. We see that the background does change only with order ϵ. We also get a rapid growth in the curvature spectrum, which can account for a higher concentration of PBHs.

Contents

Notation

In this thesis, we use the following conventions:

- We work in natural units: $c = \hbar = 1$,
- We set the reduces Planck mass to one: $M_p = 1$,
- We use the sign convention for the Minkowski metric $\eta_{\mu\nu}$: $(-1, +1, +1, +1)$,
- We use the Einstein summation convention,
- We use Greek indices for values $\mu, \nu, \rho, \sigma = 0, 1, 2, 3$ and Latin indices for $i, j = 1, 2, 3$.

Chapter 1

Introduction

Cosmology aims to describe the origin and evolution of the universe, and while much has been learned about this the last couple of decades, there are still many questions left to be answered. Some of these questions are about one of the most speculated about eras in the universe: the era of inflation. Adding an era of inflation to the conventional Big Bang model solves the *Horizon* and *Flatness* problems, which both describe the need for extremely fine-tuned initial conditions to give rise to the current universe. Furthermore, inflation gives an explanation for the origin of the Large Scale Structure (LSS). Besides creating seeds for this LSS, inflation can also predict the existence of a certain kind of dark matter, namely Primordial Black Holes (PBHs).

In this thesis we first introduce the concept of Dark Matter, the prime candidate for dark matter, the WIMP (weakly interacting massive particle), and the reason why the existence of primordial black holes is still a scenario to take seriously. After that the concept of classical inflation is introduced and the most used model and tools to describe it are presented. Then we will add quantum fluctuations and their evolution to this model. In order to achieve this, we need to explain the Slow-Roll model, and when and why it breaks down, and add some statistics for comparison with observations. Finally we will have all we need to discuss the results of this thesis, and compare them to earlier research.

1.1 Dark Matter

These times are exciting times to be a cosmologist. New measuring techniques give new insights into the cosmos that possibly ask for new physics. One of the biggest unanswered questions in cosmology today is that of dark matter. In this chapter we will explain why it is not known what dark matter is, when we are quite sure of its existence and why there is a new interest in this field. We start with a short history of dark matter.

1.1.1 History

In this section we closely follow [1, 2].
The history of dark matter is longer than one might imagine. Already around the year 1900 there were mentions of dark bodies in the universe that were needed to make sense of it. An early dynamical estimate of the percentage of dark matter in the Milky Way was done by Lord Kelvin in 1904 in his lecture notes [3]. He came to this estimate by treating the stars in the Milky Way as particles in a gas. By looking at the observed velocities of the stars, he also got an upper limit for the density of stars within a certain volume. While this was arguably a different question from what we are dealing with now,

thinking about this extra, unseen matter can been thought of as the first baby steps in this direction. Henri Poincaré reacted to this, using the phrase "matière obscure" (dark matter in English) for the first time, by saying that by Kelvin's predictions there should be little to no dark matter [1]. In respectively 1922 and 1933 the Dutch physicists Jacobus Kapteyn and his student Jan Oort also published important works about the amount of dark matter in the Milky Way, while in England James Jeans was working on the subject too. Up until this point, astronomers were still thinking of very faint stars, meteoric and nebulous matter, whose densities could be obtained by extrapolation from the luminous matter. In the next few decades, this changed.

In the 1930's, papers by multiple authors began to appear in which findings of large discrepancies between the mass of a galaxy calculated by observing visible matter and calculated by looking at the velocity dispersion were covered[4, 5, 6]. The most known of these is by Fritz Zwicky. He studied the Coma Cluster using data from Edwin Hubble and Milton Humason [7], and compared its velocity dispersion to the theoretical one, and found a huge mass discrepancy. From this he concluded that there is much more dark matter than luminous matter, but just like Oort and Kapteyn thought this was ordinary non-luminous matter: "We must know how much dark matter is incorporated in nebulae in the form of cool and cold stars, macroscopic and microscopic solid bodies, and gases."[8, p. 218] This discrepancy was not immediately accepted as a reason for the existence of dark matter by the scientific community. Instead, after more studies on clusters of galaxies, other possibilities were proposed. For example, Viktor Ambartsumian proposed that the velocity dispersion was high due to galaxies that were not part of a stable cluster, whereas Zwicky assumed that the cluster would be in equilibrium. However, in that case the lifetime of the clusters would be much less than the lifetime of the universe, which also contradicts observations. In 1961, at a conference in Santa Barbara, the conclusion was that both solutions were far from perfect and more information was needed. In the following decades many theories were introduced, but there were not enough constraints to rule them out.

In the 1970's, with the help of the 21-cm line and radio astronomy, astronomers began to notice something strange: the rotation curves of galaxies were flat, when they were expected to decline (see figure 1.1). In the famous study of Vera Rubin and Kent Ford, in which they did spectroscopic measurements of the rotation of the Andromeda Nebula, it was found that the velocity as a function of the radius was almost constant. They did not draw the conclusion that there must be dark matter, but these kind of arguments were the ones that would later finally start to convince the scientific community of the existence of dark matter. But we need to keep in mind that, at this time, the astronomers that worked on the rotation curves were mostly not the ones that worked on the velocity dispersion. In both fields, the findings were not seen as conclusive evidence for the existence of dark matter, and as such, there was no consensus about the interpretation of all these data.

This changed when due to the downfall of the steady state universe theory and the observation of quasars, cosmology as a field sparked new interest and combined Einstein's General Relativity and astrophysics. Theoretical cosmologists were pondering the question of an open/closed universe, and argued from a philosophical standpoint, that they would like it to be closed. However, for the universe to be closed, it needed to have a mass density of two orders of magnitude higher than it seemed to have. So cosmologists went looking for this extra mass, and finally the flat rotation curves and mass discrepancy came together.

In 1974, two papers [10, 11] were published in which the two results were both mentioned as reasons to believe in this unseen mass. The flat rotation curves and mass discrepancy

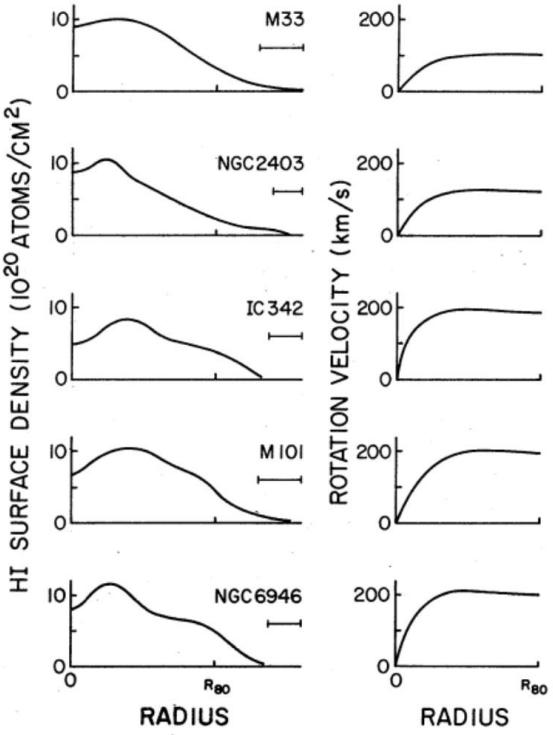

Figure 1.1: Rotation curves side by side with the azimuthally averaged hydrogen surface densities, which were thought to be a measure of the total mass density. [9]

were now seen as more a solution than a problem, it was evidence of the missing mass that was needed for the more philosophical point of a closed universe. Since then, most of the scientific community has been convinced there is some missing mass, or dark matter.

At first, it was thought that dark matter was just non-luminous matter, for example dust or gas clouds. However, these clouds would be visible when blocking the light of stars. Furthermore, the theory of nucleosynthesis predicts the abundance of the elements given a certain abundance of baryons. From the abundances of elements like helium and lithium, it is found that baryonic matter can only make up about a sixth of the matter in the universe.

Since the seventies, more evidence of dark matter has been found, most notably in the Cosmic Microwave Background (CMB). Two telescopes (WMAP and Planck) measured the relic photons from the time of recombination. Analysing the power spectrum obtained from these measurements gives a ratio of cold dark matter to ordinary matter of about five to one.

So while in the beginning of this story the term “dark matter” was used for non-luminous matter, we see that currently Dark Matter is understood to be the unknown biggest part of the universes matter density. The current definition no longer includes matter such as meteors or cold stars. There are a couple of candidates that have been considered the last couple of decades, mostly in the form of new particles. We will not go into detail for most of them here, but let us mention what was the top candidate for some time.

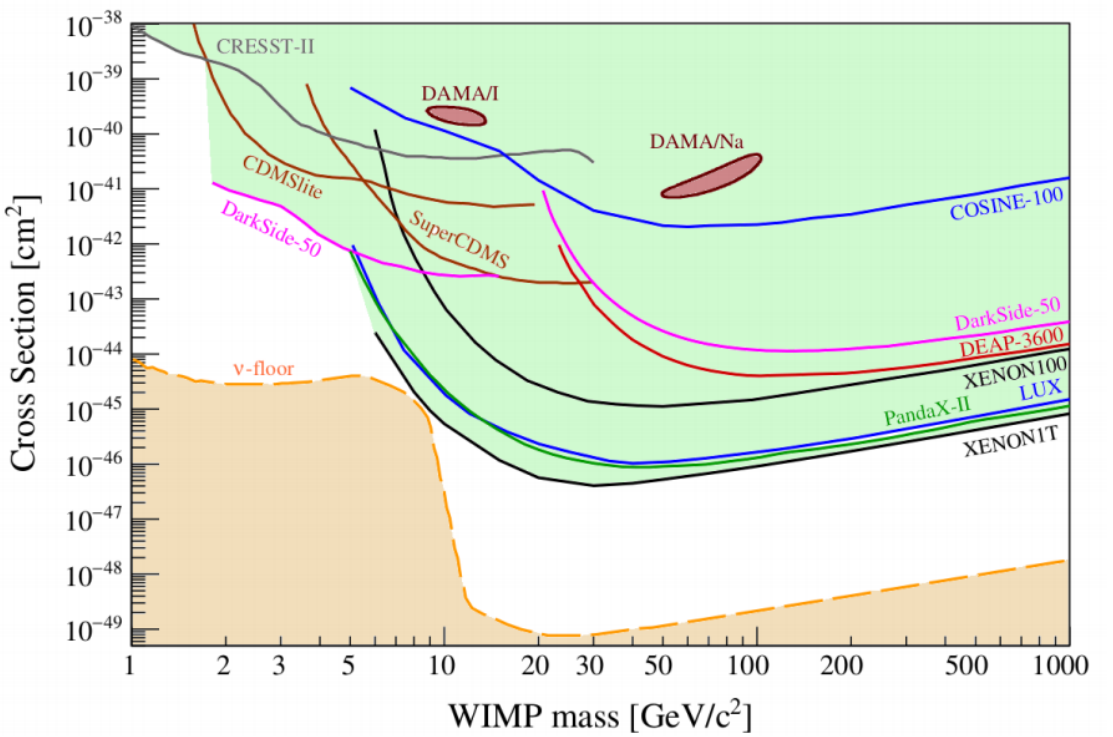

Figure 1.2: Exclusion plot of the search for the spin-independent WIMP-nucleon cross sections. The green shaded region is the region excluded by direct observation experiments, while the orange shaded region is the "neutrino floor", the bound of the possibility of measuring the WIMP before it gets obscured by the irreducible background from coherent neutrino-nucleus scattering. Figure is taken from 'Direct Detection of WIMP Dark Matter: Concepts and Status' [13].

1.1.2 WIMPs

Currently it is estimated that 85% of the matter in the universe is dark matter. We can divide the different candidates for dark matter into cold dark matter and hot dark matter. Hot dark matter consists of particles that move with almost the speed of light, while cold dark matter moves slowly in comparison with the speed of light. Cold dark matter (CDM) is also useful to explain the forming of structures.

For a long time it was widely believed that Weakly Interacting Massive Particles (WIMPs) would be the answer to the question of dark matter. These hypothetical particles interact gravitationally and through the weak force with other matter. For the WIMPs to be a cold relic from thermal decoupling, there is a lower bound on its mass of a few keV.[12] Furthermore, if we assume thermal production, we know from the observed dark matter density the rate with which the particles self-annihilate must have a cross section of the order of $10^{-26}\text{cm}^3/s$. With Super-Symmetric arguments, a particle that interacted only gravitationally and with the weak force with exactly these two features was predicted to exist. This came to be known as the 'WIMP miracle'. Immediately experiments were set up to look for this particle, but as more time goes by, it becomes more and more probable that we are not going to find it, see figure 1.2. This failure to find WIMPs caused renewed interest in other dark matter candidates, like Primordial Black Holes (PBH).

1.1.3 Primordial black holes

So dark matter might be (partly) made up from primordial black holes. What do we know about primordial black holes, and how can we find them?

While currently Black Holes can only be created out of the explosion of heavy stars, in the early universe, the density of the universe was much higher, and therefore Black Holes could be generated by relatively small density fluctuations. The existence of such black holes was first predicted by Zel'dovich and Novikov in their 1966 paper [14]. At this time, the term 'black hole' was not yet used, but they mention singularities and Schwarzschild radii in the early universe. In 1970, a paper by Stephen Hawking was published, in which he predicted that a large number of objects with masses from 10^{-5}g upwards could have been created in the early universe due to density fluctuations [15]. Currently, we know that these smallest PBHs, up to 10^{15}g, must have evaporated due to Hawking radiation, and are therefore not present in the current universe.

In 1996 a paper was published, in which the formation of PBH due to an inflationary period in the universe was proposed [16]. A PBH is formed in the early radiation-dominated universe, when an overdensity of about $\frac{\delta\rho}{\rho} = \mathcal{O}(1)$ causes a region to gravitationally collapse into a black hole. Such a black hole will then have the same mass as the mass contained in the collapsed region. For this collapse to happen, we need sharp peaks in the primordial power spectrum. This can possibly happen in some inflationary models, from which we will discuss one in this thesis.
In figure 1.3 it is shown that there are still two windows open for PBH to make up most (or all, if we for example consider broad peaks) of the universe's dark matter: between $10^{-13}M_{\mathrm{PBH}}/M_{\odot}$ and $10^{-8}M_{\mathrm{PBH}}/M_{\odot}$, where it was thought to have been constrained by neutron star capture and around $10^{2}M_{\mathrm{PBH}}/M_{\odot}$.

This divides the search for PBH as dark matter in roughly two cases: massive primordial black holes and low mass primordial black holes. The massive PBHs are used to explain the super-massive black holes in the centre of galaxies, and other black holes that are more massive than the general big bang model predicts, as measured by LIGO. These massive PBH are created by high or broad peaks in the primordial power spectrum. These high peaks collapse into massive black holes when re-entering the horizon. The broad peaks, however, can first collapse and form clusters of black holes, which later merge and accrete more mass. These massive black holes then also function as seeds for LSS. [17]

As we have now seen, the existence of PBHs can answer some big questions. But for these PBHs to be created, there have to be large and/or broad peaks in the primordial power spectrum. In this thesis, we explore one way in which the peaks of the primordial power spectrum rapidly grow and therefore create the PBHs.

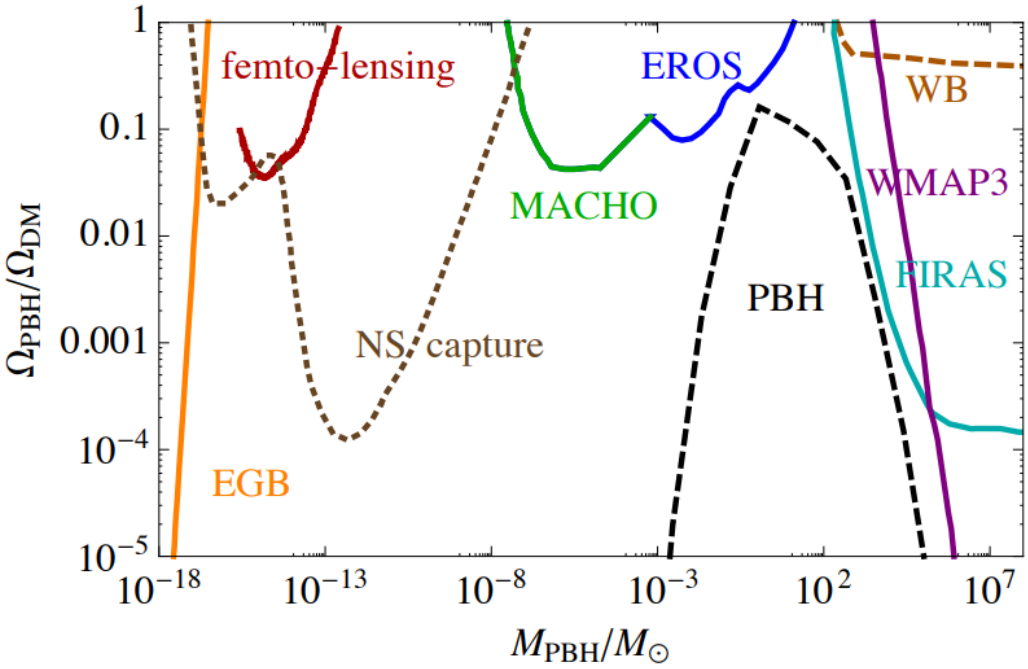

Figure 1.3: Constraints on the abundances of primordial black holes in the current universe. Shown are constraints obtained by: extra galactic background photons (EGB, orange), femto-lensing observations (Femto-lensing, red), micro-lensing observations (MACHO and EROS, green and blue), fluctuations in the CMB (FIRAS and WMAP3, cyan an purple) and observations on wide binaries (WB, brown). The brown, dotted line with NS was thought to be constrained by star formation and capture by neutron stars, but this is currently being debated. The black dotted line corresponds to a particular scenario of PBH formation as proposed by [17].

Chapter 2

Inflation

To understand and describe the way primordial black holes are generated, we need to understand the mechanism of inflation. In this chapter we will explain why we need inflation, and introduce the language with which we can describe it. (We largely follow the Baumann lectures on inflation[18] and Weinberg's book 'Cosmology' [19].)

2.1 Classical Inflation

Cosmic inflation is a period of exponential expansion around 10^{-34} seconds after the Big Bang. It is created as the solution to the horizon and the flatness problem. When we look at a picture (figure 2.1) of the Cosmic Microwave Background (CMB) we can see two things: for one, the universe looks the same in all directions, but secondly, there are small fluctuations from the average temperature. It is thought that cosmic inflation is responsible for both the homogeneity and the small perturbations that will later form the large scale structure of the universe.

During inflation, the comoving Hubble horizon shrinks. This way, small perturbations that were once inside the horizon, get stretched to larger scales to become frozen outside the horizon. Later, when the universe is again expanding normally, these perturbation enter the horizon again, and cause collapses into galaxies and galaxy clusters.

From observations, it is not unreasonable to assume we live in both an homogeneous and isotropic universe. This assumption that the universe should look the same for all observers is called the cosmological principle. The metric for the space time of such an universe is given by the Friedmann–Lemaître–Robertson–Walker (FLRW) metric:

$$ds^2 = -dt^2 + a^2(t)\left(\frac{dr^2}{1-\kappa r^2} + r^2\left(d\theta^2 + \sin^2(\theta)d\phi^2\right)\right), \tag{2.1}$$

where $a(t)$ is the scale factor, κ the curvature parameter ($+1, 0, -1$ for a positively curved, flat, negatively curved universe respectively) and we use comoving coordinates. Comoving coordinates mean that while the universe expands with an increasing scale factor a, a particle with no acting forces upon it, will keep the same coordinates. An important parameter that characterizes such an universe is the Hubble parameter

$$H = \frac{\dot{a}}{a} \tag{2.2}$$

which parametrizes the expansion rate of the universe. It is positive for an expanding universe and negative for a collapsing one. It also sets the fundamental scales: the Hubble time $t = H^{-1}$ and the Hubble length $d = H^{-1}$. In different stages of the evolution of the

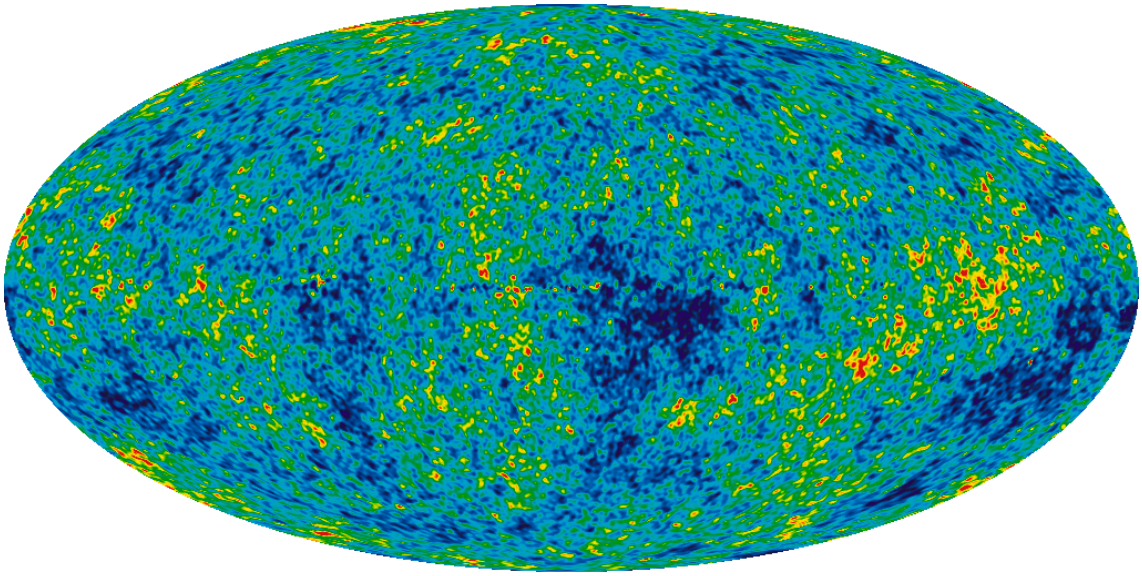

Figure 2.1: Nine years of WMAP data give this picture of the Cosmic Microwave Background (CMB). The CMB is made up of relic photons from the time when radiation decoupled from matter. The colour differences show the temperature fluctuations (±200 microKelvin) which correspond to the seeds of LSS. Credit: NASA/WMAP Science Team

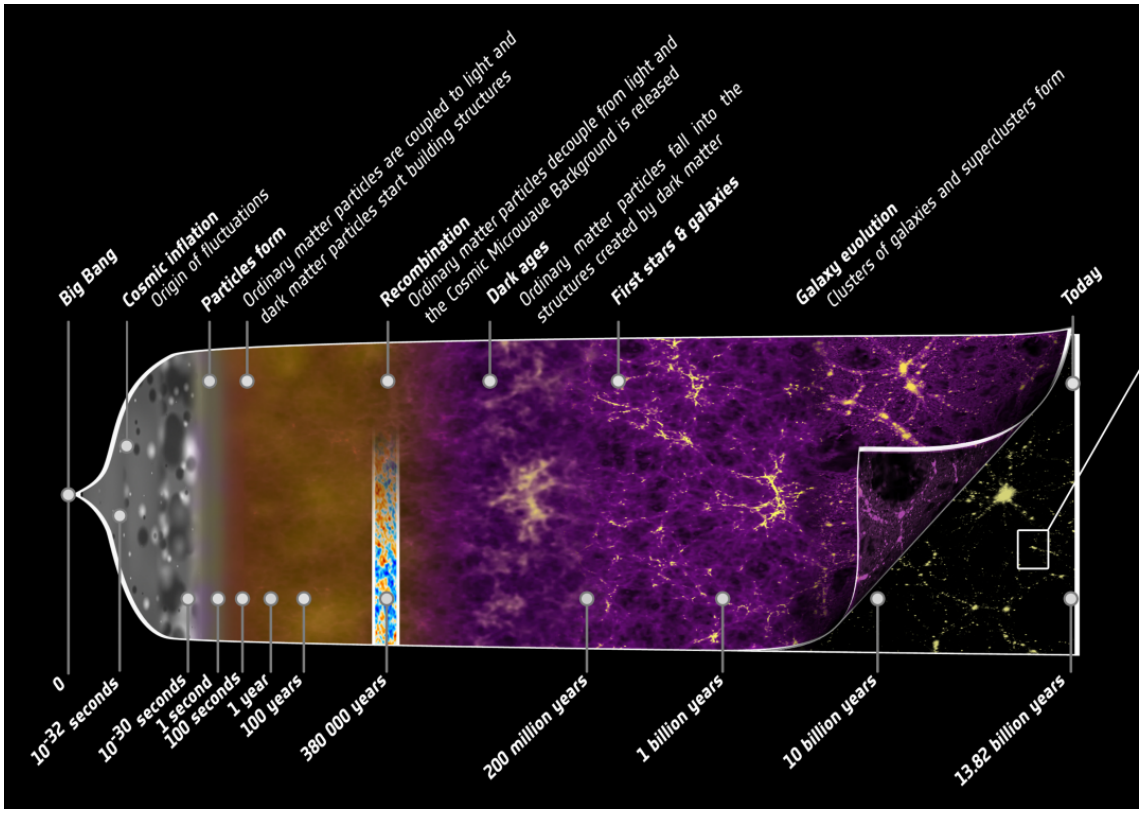

Figure 2.2: A summary of the history of the universe. Inflation happens here at $10^{-32}s$, after which the radiation era begins. During inflation the quantum fluctuations are created which will seed the Large Scale Structure (for example galaxy clusters) we can see in later times. Image source: NASA Planck project

universe, the scale factor and the Hubble parameter had different shapes, depending on the dominant energy (radiation, matter, dark matter, etc.).

It is convenient to describe inflation in conformal time

$$\tau \equiv \int \frac{dt}{a(t)}, \tag{2.3}$$

which changes the FLRW metric 2.1 to

$$ds^2 = a^2(\tau)\left(-d\tau^2 + \frac{dr^2}{1-\kappa r^2} + r^2\left(d\theta^2 + \sin^2(\theta)d\phi^2\right)\right). \tag{2.4}$$

The use of conformal time will let us describe the light cone at the time as straight lines at a 45° angle. We then also introduce the conformal Hubble parameter

$$\mathcal{H} = \frac{a'}{a} = \frac{\partial_\tau a}{a} = \frac{a\partial_t a}{a} = aH. \tag{2.5}$$

The comoving particle horizon is defined as the maximum comoving distance a photon can travel between some initial time, t_i, (often the origin of the universe, defined by $a(t_\mathrm{i} = 0) = 0$) and some end time, t_e,

$$\chi_p(\tau) \equiv \int_{t_\mathrm{i}}^{t_\mathrm{e}} \frac{dt}{a(t)} = \tau_\mathrm{e} - \tau_\mathrm{i}. \tag{2.6}$$

This comoving particle horizon also gives the distance over which causal contact can have been realized, and is therefore important in one of the biggest puzzles in cosmology, *the horizon problem*, which we will explain later on. We can also convert this to the physical distance by multiplying by the scale factor: $d_p(t) = a(t)\chi_p$.
Another horizon that is physically important is the event horizon, this gives the distance so that there cannot be any causal contact in the future and is defined as

$$\chi_\mathrm{e} = \int_\tau^{\tau_\mathrm{max}} d\tau = \tau_\mathrm{max} - \tau, \tag{2.7}$$

where τ_max is the 'end of time'.

2.2 Dynamics

Now we have the means to describe some of the dynamics of inflation. The universe as described by the FLRW metric 2.1 should obey the Einstein equation,

$$G_{\mu\nu} = 8\pi G T_{\mu\nu} \tag{2.8}$$

where $G_{\mu\nu}$ is the Einstein tensor

$$G_{\mu\nu} \equiv R_{\mu\nu} - \frac{1}{2}g_{\mu\nu}R, \tag{2.9}$$

$$\tag{2.10}$$

with the Ricci tensor en scalar given by,

$$R_{\mu\nu} = \partial_\rho \Gamma^\rho_{\mu\nu} - \partial_\nu \Gamma^\rho_{\rho\mu} + \Gamma^\rho_{\rho\lambda}\Gamma^\lambda_{\mu\nu} - \Gamma^\rho_{\nu\lambda}\Gamma^\lambda_{\rho\mu}, \quad R = g^{\mu\nu}R_{\mu\nu}, \tag{2.11}$$

and $T_{\mu\nu}$ is the stress-energy tensor. Now we have to define such a tensor. Let us start with defining the timelike four-velocity vector $u^\mu \equiv \frac{dx^\mu}{d\tau}$ such that $g_{\mu\nu}u^\mu u^\nu = -1$. We also define a tensor $\gamma_{\mu\nu} = g_{\mu\nu} + u_\mu u_\nu$, the matter energy density $\rho = T_{\mu\nu}u^\mu$, the isotropic pressure $p = \frac{1}{3}T_{\mu\nu}\gamma^{\mu\nu}$, the energy–flux vector $q_\mu = -\gamma^\alpha_\mu T_{\alpha\beta}u^\beta$ and the symmetric and trace-free anisotropic stress tensor $\Sigma_{\mu\nu} = \gamma^\alpha_{\langle\mu}\gamma^\beta_{\nu\rangle}T_{\alpha\beta}$. Now we write the energy-momentum tensor of a general fluid as

$$T_{\mu\nu} = \rho u_\mu u_\nu + p\gamma_{\mu\nu} + 2q_{(\mu}u_{\nu)} + \Sigma_{\mu\nu}. \tag{2.12}$$

In the special case of the perfect fluid (where there is no viscosity, shear stress or heat conduction) there exists a unique 4-velocity such that $\Sigma_{\mu\nu} = q_\mu = 0$,

$$T^\mu_\nu = g^{\mu\alpha}T_{\alpha\nu} = (\rho + p)u^\mu u_\nu - p\delta^\mu_\nu \tag{2.13}$$

where ρ and p are the proper energy density and pressure in the fluid rest frame and u^μ is the 4-velocity of the fluid. If we move to a frame that is comoving with the fluid, we can choose $u^\mu = (1, 0, 0, 0)$, such that

$$T^\mu_\nu = \begin{pmatrix} \rho & 0 & 0 & 0 \\ 0 & -p & 0 & 0 \\ 0 & 0 & -p & 0 \\ 0 & 0 & 0 & -p \end{pmatrix}. \tag{2.14}$$

We can then put the Einstein equations in the following form, called the Friedmann equations

$$H^2 = \frac{1}{3}\rho - \frac{\kappa}{a^2} \tag{2.15}$$

$$\dot{H} + H^2 = \frac{\ddot{a}}{a} = -\frac{1}{6}(\rho + 3p). \tag{2.16}$$

When combined, these equations can be written as follows:

$$\frac{d\rho}{dt} + 3H(\rho + p) = 0 \tag{2.17}$$

$$\text{or} \tag{2.18}$$

$$\frac{d\ln\rho}{d\ln a} = -3(1 + w), \quad \text{with} \quad w \equiv \frac{p}{\rho}, \tag{2.19}$$

which is called the continuity equation. Here w is the equation of state parameter, which takes different values for different kinds of matter. For the equation of state of non-relativistic matter $w = 0$, for ultra-relativistic matter $w = \frac{1}{3}$, and for inflation $w \approx -1$. When integrated, this last equation gives us

$$\rho \propto a^{-3(1+w)}. \tag{2.20}$$

Now we can read off the time evolution of the scale factor for different kind of universes.

$$a(t) \propto \begin{cases} t^{2/3(1+w)} & w \neq -1 \\ e^{Ht} & w \approx -1 \end{cases} \tag{2.21}$$

For a universe that is flat ($\kappa = 0$) and dominated by

- non-relativistic matter ($w = 0$) the scale factor goes as $a \propto t^{2/3}$
- radiation or relativistic matter ($w = \frac{1}{3}$) the scale factor goes as $a \propto t^{1/3}$

- a cosmological constant ($w = -1$) the scale factor goes as $a \propto e^{Ht}$

While it is not completely necessary for a physical model, most physicists would like the universe not to be a product of special, fine-tuned initial conditions. The conventional Big Bang model needed these special, fine-tuned initial conditions to predict the universe that we know and love today. There are two 'problems' of initial conditions that inflation solves: the horizon problem/initial homogeneity problem and the flatness problem/initial velocities problem. These are not inconsistencies in the standard cosmological model, but rather shortcomings in its predictive power.

The first problem arises for example when we look at the CMB. We see that at the moment the photons decoupled from matter, the inhomogeneities were much smaller than they are now. This makes sense, because these inhomogeneities are unstable because of the gravitational force and will therefore grow. But it follows, that at the time before the CMB, the universe should contain even smaller inhomogeneities. How can our universe be so smooth? Even when in the original Big Bang model, different patches of the CMB are causally disconnected? This is called the *horizon problem*.

The second problem is called the *flatness problem*. Observations show that the universe today is near-flat. To better show the problem, we then write the Friedmann equation as

$$1 - \Omega(a) = \frac{-\kappa}{(aH)^2} \tag{2.22}$$

$$\tag{2.23}$$

where

$$\Omega(a) \equiv \frac{\rho(a)}{\rho_{\text{crit}}(a)}, \quad \text{and} \quad \rho_{\text{crit}} \equiv \frac{3H^2}{8\pi G}. \tag{2.24}$$

As the comoving Hubble radius $(aH)^{-1}$ grows with time, $|\Omega - 1|$ must diverge with time. As we know, the universe is near-flat now so $\Omega \sim 1$, but $\Omega = 1$ is a unstable fixed point. So for Ω to be so close to 1 today, it should have been even closer to 1 in the early universe. Why would this be the case?

The answer to both of these question is (obvious by the title of this chapter): inflation. Both of the problems arise because the comoving Hubble radius is strictly increasing, so the idea is that they can be solved by assuming a model in which the Hubble radius decreases for some time. During inflation the Hubble parameter H is approximately constant and the scale factor a grows exponentially. The comoving Hubble radius $(aH)^{-1}$ does indeed decrease for these a and H, but the particle horizon (or conformal time) still grows. Now $\Omega = 1$ is an attractor instead of a unstable fixed point. And patches of the CMB that are not in causal contact now, have been in causal contact before inflation, and can therefore have had the time to form a homogeneous universe (see figure 2.3).

This period of shrinking of the Hubble radius also explains how quantum fluctuations can exit the horizon during inflation and re-enter the horizon after inflation to then gravitationally collapse to form large-scale structure or primordial black holes.

The Friedmann equations relate the following equivalent conditions for inflation:

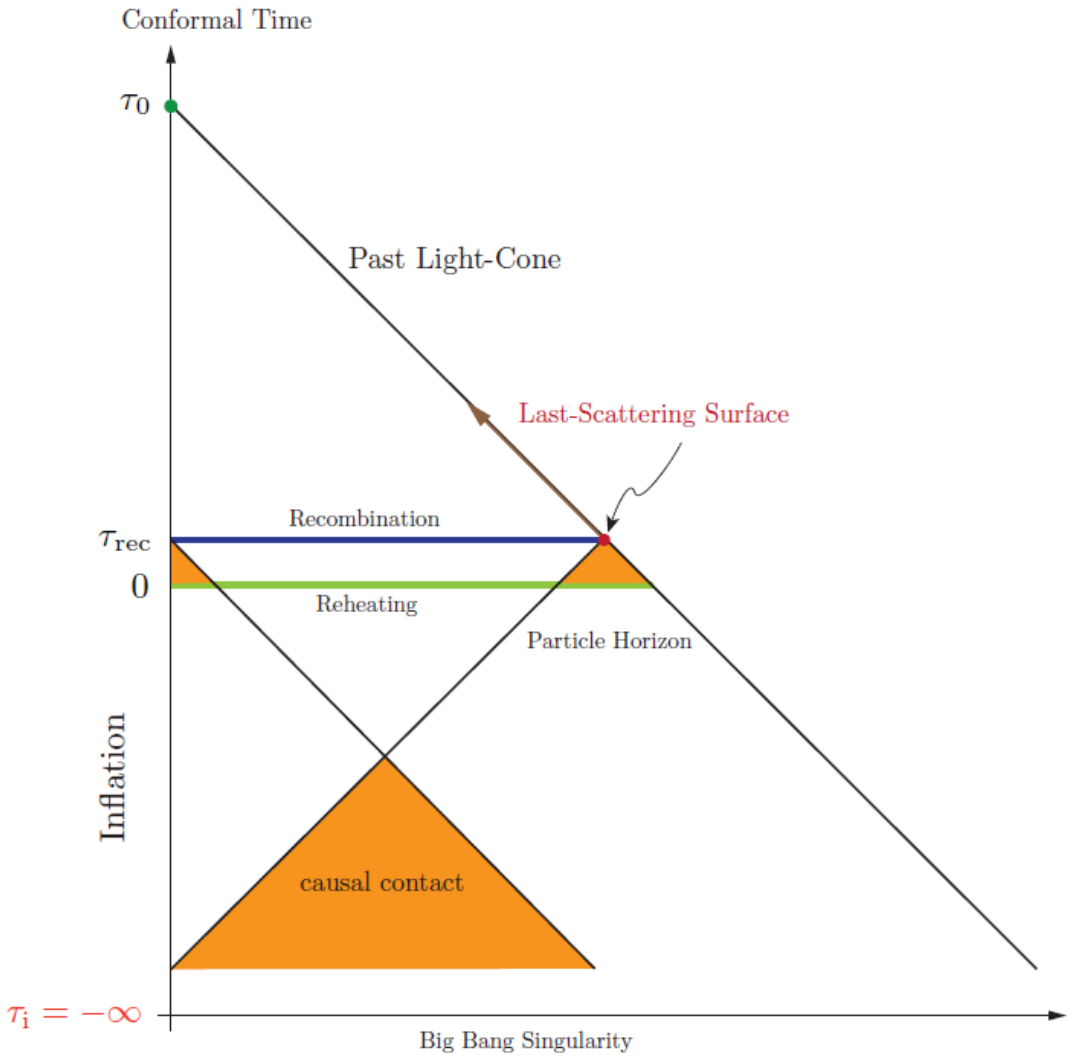

Figure 2.3: In conformal time, the light cone consists of straight lines in a 45° angle with the time direction. In conventional big bang models, $a \propto \tau$ or $a \propto \tau^2$ everywhere. Then the Big Bang happened at $a = 0 \implies \tau = 0$. This means that two patches far enough apart at recombination have never been in causal contact. If we add a period of inflation, we extend the conformal time from 0 to $-\infty$. This way, the point where $\tau = 0$ is actually the end of inflation, and patches far apart at the time of recombination have been in causal contact somewhere during inflation.

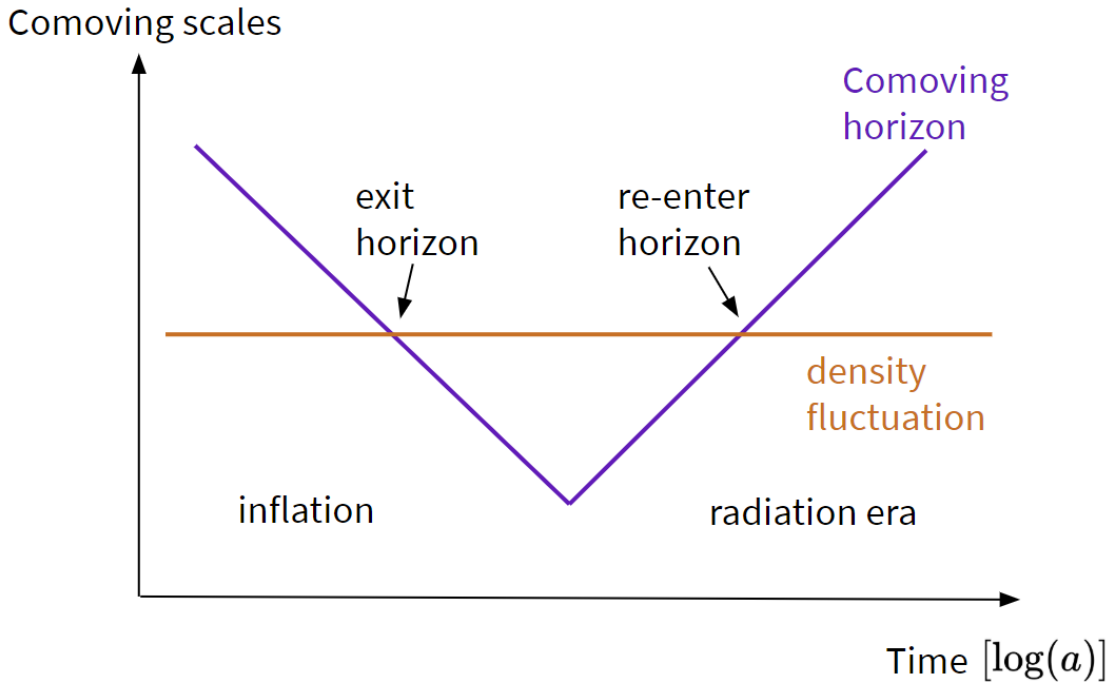

Figure 2.4: Inflation can make perturbation that have been created quantum-mechanically, exit the horizon, and later re-enter it. These perturbations will keep the same comoving length, but their physical length will grow with $l_{\text{physical}} = a l_{\text{comoving}}$

$$\frac{d}{dt}(\frac{1}{aH}) < 0 \tag{2.25}$$

$$\frac{d^2a}{dt^2} > 0 \tag{2.26}$$

$$p < -\frac{1}{3}\rho. \tag{2.27}$$

In this thesis, the second condition is the most important. We can express the second time derivative of the scale factor in terms of the Hubble parameter and it's time derivative

$$\frac{\ddot{a}}{a} = H^2(1-\epsilon_1), \quad \text{where} \quad \epsilon_1 \equiv -\frac{\dot{H}}{H^2}. \tag{2.28}$$

We call ϵ_1 the first Slow-Roll parameter and it plays an important role in this thesis, this will be explained further in the section about Slow-Roll. With these expressions we can also express the second condition as follows

$$\epsilon_1 = -\frac{d\ln H}{dN} < 1, \tag{2.29}$$

where N is the number of e-folds $N = \ln a$.

There is an infinite number of possible models of inflation, but we will only use and therefore focus on the simplest models: the models with a single scalar field ϕ called the 'inflaton'. The action of the system with such a field minimally coupled to gravity is as follows

$$S = \frac{1}{8\pi G}\int d^4x\sqrt{-g}(\frac{1}{2}R + \frac{1}{2}g^{\mu\nu}\partial_\mu\phi\partial_\nu\phi - V(\phi)), \tag{2.30}$$

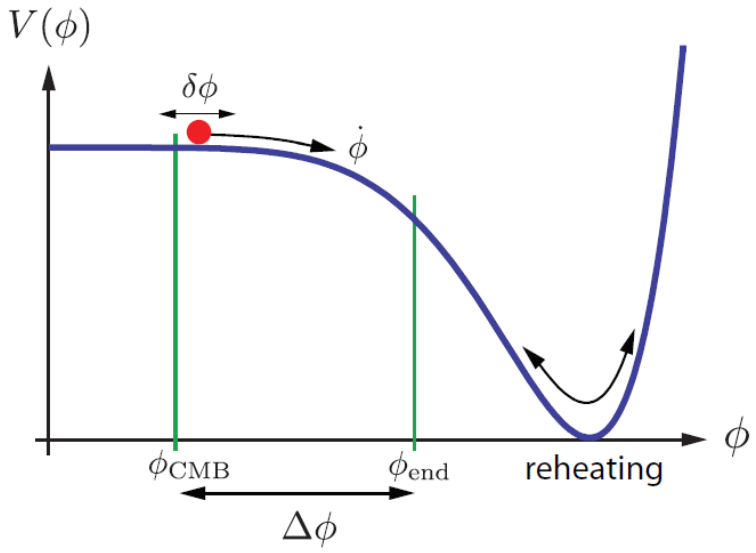

Figure 2.5: Example of a inflaton potential.

where the potential, $V(\phi)$, describes the self-interaction of the inflaton-field. In subsequent equations we will put $8\pi G = 1$. From this we determine the energy-momentum tensor for the inflaton

$$T^{(\phi)}_{\mu\nu} \equiv -\frac{2}{\sqrt{-g}}\frac{\delta S_\phi}{\delta g^{\mu\nu}} - \partial_\mu\phi\partial_\nu\phi - g_{\mu\nu}(\frac{1}{2}\partial^\sigma\phi\partial_\sigma\phi + V(\phi)), \tag{2.31}$$

and the equation of motion

$$\frac{\delta S_\phi}{\delta\phi} = \frac{1}{\sqrt{-g}}\partial_\mu(\sqrt{-g}\partial^\mu\phi) + \frac{dV}{d\phi} = 0. \tag{2.32}$$

If we assume the FLRW metric 2.1 and a homogeneous field $\phi(t,\vec{x}) = \phi(t)$, the energy-momentum tensor again reduces to the one for a perfect fluid, with

$$\rho_\phi = \frac{1}{2}\dot{\phi}^2 + V(\phi) \tag{2.33}$$

$$p_\phi = \frac{1}{2}\dot{\phi}^2 - V(\phi). \tag{2.34}$$

Which results in the equation of state

$$w_\phi = \frac{\frac{1}{2}\dot{\phi}^2 - V(\phi)}{\frac{1}{2}\dot{\phi}^2 + V(\phi)}. \tag{2.35}$$

This shows that when $V > \frac{1}{2}\dot{\phi}^2$ the scalar field can induce a negative pressure ($w_\phi < 0$) and accelerated expansion ($w_\phi < -\frac{1}{3}$). If we use the FLRW metric 2.1, we find that equation 2.32 becomes

$$\ddot{\phi} + 3H\dot{\phi} + \frac{dV}{d\phi} = 0 \tag{2.36}$$

$$H^2 = \frac{1}{3}(\frac{1}{2}\dot{\phi}^2 + V(\phi)). \tag{2.37}$$

These equations do not always give rise to inflation, but when the first slow-roll parameter is smaller that 1, we enter the Slow-Roll regime, which does give inflation.

2.3 Slow-Roll Inflation

In the last section we introduced the Slow-Roll parameter ϵ_1, we will now explain what Slow-Roll is and why it is important.
Inflation or accelerated expansion occurs when the first Slow-Roll parameter is small ($\epsilon_1 < 1$) and ends when this condition is violated ($\epsilon_1 = 1$). During Slow-Roll inflation, the first and second Slow-Roll parameter are small $\epsilon_1, |\epsilon_2| \ll 1$. We can therefore neglect all order ϵ_1^2 and ϵ_2^2 corrections to our equations. This happens when the potential $V(\phi)$ is almost flat, and the potential energy is much larger than the kinetic energy $V(\phi) < \frac{1}{2}\dot{\phi}^2$. This reduces the equation of motion to

$$3H\dot{\phi} + \frac{dV}{d\phi} \approx 0. \tag{2.38}$$

Remember how the first Slow-Roll parameter is defined:

$$\epsilon_1 \equiv -\frac{\dot{H}}{H^2} = -\partial_N \ln(H). \tag{2.39}$$

The second Slow-Roll parameter is measure of rate of change of the first Slow-Roll parameter and defined as

$$\epsilon_2 \equiv \dot{\epsilon}_1/(H\epsilon_1) = 2\ddot{\phi}/(\dot{\phi}H) + 2\epsilon_1 = \frac{\epsilon_1'}{\epsilon_1 \mathcal{H}} = \partial_N \ln(\epsilon_1) \tag{2.40}$$

Smallness of this second SR parameter will ensure that the period of accelerated expansion can last long enough to solve the horizon and flatness problems. The Slow-Roll conditions are therefore $|\epsilon_2|, \epsilon_1 \ll 1$.

Slow-roll inflation is an attractor, this means that when the potential supports SR inflation, all potential solutions rapidly approach each other. Therefore the universe, as it exits SR inflation, is independent on the initial conditions of SR inflation. [20] This, therefore, also solves problems of fine-tuning.

We can calculate the number of e-foldings between two time points during inflation by integrating the Hubble Parameter over time

$$N \equiv \ln a_2 - \ln a_1 \tag{2.41}$$

$$= \int_{t_1}^{t_2} H dt = \int_{\tau_1}^{\tau_2} \mathcal{H} d\tau. \tag{2.42}$$

To solve our problems we need the number of e-foldings to be around 60. This gives for the total of e-foldings during inflation

$$N_{total} = \ln a_{\text{end}} - \ln a_{\text{start}} = \int_{t_{\text{start}}}^{t_{\text{end}}} H dt = \int_{\tau_{\text{start}}}^{\tau_{\text{end}}} \mathcal{H} d\tau \gtrapprox 60. \tag{2.43}$$

As we have seen, slow-roll inflation ends when $\epsilon_1 = 1$, in other words when the potential becomes too steep, but there is another ending possible: the potential can become too flat for the SR approximation to apply. When this happens, we enter a new regime: Ultra-slow-roll inflation.

2.4 Ultra-Slow-Roll Inflation

When the potential becomes flat, we can no longer neglect the contribution of the potential to the equation of motion. What happens instead, is that the second derivative of the inflation field becomes increasingly small. This way, the equation of motion reduces to

$$\ddot{\phi} + 3H\dot{\phi} \approx 0. \tag{2.44}$$

If we stay in the SR approximation when the potential becomes increasingly flat, the kinetic density of the inflaton field would reduce faster that it would in free fall. This is not possible, and therefore we need a new regime. In USR the kinetic density decreases as if in free fall. USR ends when $\ddot{\phi}$ is again in the same order of magnitude as the slope of the potential, or when inflation ends for another reason.[21]

During USR, the first SR parameter is still smaller than 1, so we are still in the inflation era, but this does no longer apply for the second SR parameter. When the potential is flat enough, quantum kicks against the inflaton will be significant. For the slow-roll parameters, this means that while ϵ_1 is much smaller than 1, ϵ_2 is not smaller than 1. This will change our approximations significantly.

The second SR parameter is, during USR, given by [22]

$$\epsilon_2 \equiv \frac{\partial}{\partial N} \ln(\epsilon_1) = -6 + 2\epsilon_1, \tag{2.45}$$

this means that $\epsilon_2 \approx -6$ as $\epsilon_1 \ll 1$ during USR. We can also define 3rd, 4th, etc. SR parameters as follows:

$$\epsilon_n \equiv \frac{\partial}{\partial N} \ln(\epsilon_{n-1}) = \frac{1}{\epsilon_{n-1}} \frac{\partial \epsilon_{n-1}}{\partial N}$$

when we calculate this, we see

$$\epsilon_n = 2\epsilon_1 \qquad \text{for} \quad n = \text{odd} \tag{2.46}$$

$$\epsilon_n = -6 + 2\epsilon_1 \qquad \text{for} \quad n = \text{even}. \tag{2.47}$$

Chapter 3

Perturbations during Inflation

Until now we focused on classical models of inflation, but to account for the density fluctuations we should take quantum mechanics into consideration. As our inflaton field is rolling down the potential, it will experience 'quantum kicks' in both directions. While we define the field as position independent $\phi(t)$, these fluctuations do depend on the position $\delta\phi(t, \vec{x})$. These fluctuations in the field causes inflation to end earlier in the parts of the universe that received a quantum kick down the potential, and later in the parts of the universe that received a kick up the potential. The slightly different time-evolution in the different parts causes relative density fluctuations. To describe such fluctuations, we can use Linear Perturbation theory. During this section, we makes use of 'Cosmological Inflation and Large-Scale Structure' by Liddle and Lyth [23].

3.1 Linear Perturbation Theory

The leading theory for the formation of large scale structure is that of gravitational collapse. In this scenario, the universe starts out smooth. The Cosmic Microwave Background (CMB) shows us that, at the time of decoupling, the density of the universe is almost homogeneous, with small perturbations of order 10^{-5}. These density inhomogeneities cause inhomogeneities in the local space-time. The easiest way to write these inhomogeneities, is by decoupling the background value from the perturbations

$$\delta X(t, \vec{x}) \equiv X(t, \vec{x}) - \bar{X}(t), \tag{3.1}$$

were δX is the perturbation, X is the quantity that we want to split (f.e. the metric $g_{\mu\nu}$ or the density field ρ) and $\bar{X}$ the background value that does not depend on location, but only on time. We assume that these perturbations are small ($\delta X \ll X$) so that we can treat them linearly. This means, that if we expand the Einstein equation up to linear order, it gives a fairly accurate description,

$$\delta G_{\mu\nu} = 8\pi G \delta T_{\mu\nu}. \tag{3.2}$$

What we should keep in mind, is that these perturbations are Gauge dependent, and therefore cannot be seen as physical perturbations. We shall define gauge invariant (physical) perturbations later on in this chapter.

Due to the symmetries of the background spacetime, we can perform SVT (scalar, vector, tensor) decomposition. When we have done this, we can independently treat the scalar, vector and tensor components of the metric and stress-energy perturbations. This is easiest seen in their Fourier form

$$\delta X_{\vec{k}}(t) = \int d^3\vec{x} e^{i\vec{k}\cdot\vec{x}} \delta X(t, \vec{x}), \tag{3.3}$$

where the different Fourier modes do not interact, and can therefore be studied independently. This often makes the differential equations much easier to solve. A perturbation also has some helicity, which differs between scalars, vectors and tensors, defined by

$$X_{\vec{k}} \to e^{im\theta} X_{\vec{k}} \tag{3.4}$$

where m is the helicity (0, ± 1 and ± 2 for scalars, vectors and tensors respectively) and θ the angle under which the coordinate system is rotated around $\vec{k}$.

So let us define the perturbations for the inflaton and the metric,

$$\delta\phi(t, \vec{x}) = \phi(t, \vec{x}) - \bar{\phi}(x), \tag{3.5}$$
$$\delta g_{\mu\nu}(t, \vec{x}) = g_{\mu\nu}(t, \vec{x}) - \bar{g}_{\mu\nu}(x). \tag{3.6}$$

Now look at this for a moment: we know that the symmetric 4x4 tensor $g_{\mu\nu}$ has 10 degrees of freedom. With SVT decomposition we classify these into three categories: scalars, vectors and tensors. This, we can do by looking at their helicity. So lets decompose the spacetime interval into its scalar, vector and tensor parts,

$$ds^2 = g_{\mu\nu} dx^\mu dx^\nu \tag{3.7}$$
$$= -(1 + 2\Phi)dt^2 + 2aB_i dx^i dt + a^2((1 - 2\Psi)\delta_{ij} + E_{ij})dx^i dx^j, \tag{3.8}$$

where

$$B_i \equiv \partial_i B + S_i, \quad \text{with} \quad \partial^i S_i = 0, \tag{3.9}$$
$$\text{and} \tag{3.10}$$
$$E_{ij} \equiv 2\partial_{ij} E + 2\partial_{(i} F_{j)} + h_{ij}, \quad \text{with} \quad \partial^i F_i = 0, \quad \text{and} \quad h^i_i = \partial^i h_{ij} = 0. \tag{3.11}$$

Our decomposition now leaves us with

- four scalars: Φ, Ψ, E and B, describing the generalisation of Newtonian gravity,
- two vectors: S_i and F_i, describing gravito-magnetism,
- and one tensor: h_{ij}, describing gravitational waves,

which account for $4+2\times2+2 = 10$ degrees of freedom. The vector perturbations all decay, and are therefore not that useful to study. We are thus left with the scalar and tensor perturbations. While these are both interesting, in this thesis we will focus on the scalar ones, because the scalar metric perturbations couple to the scalar field perturbations $\delta\phi$, while the tensor perturbation decouple from it.

The inflaton field is the dominant energy in the universe during inflation. This also means that the perturbations in the inflaton field have a backreaction on the spacetime geometry. We can study this by looking at the perturbed Einstein equation, which describes this coupling,

$$\delta G_{\mu\nu} = 8\pi G \delta T_{\mu\nu}. \tag{3.12}$$

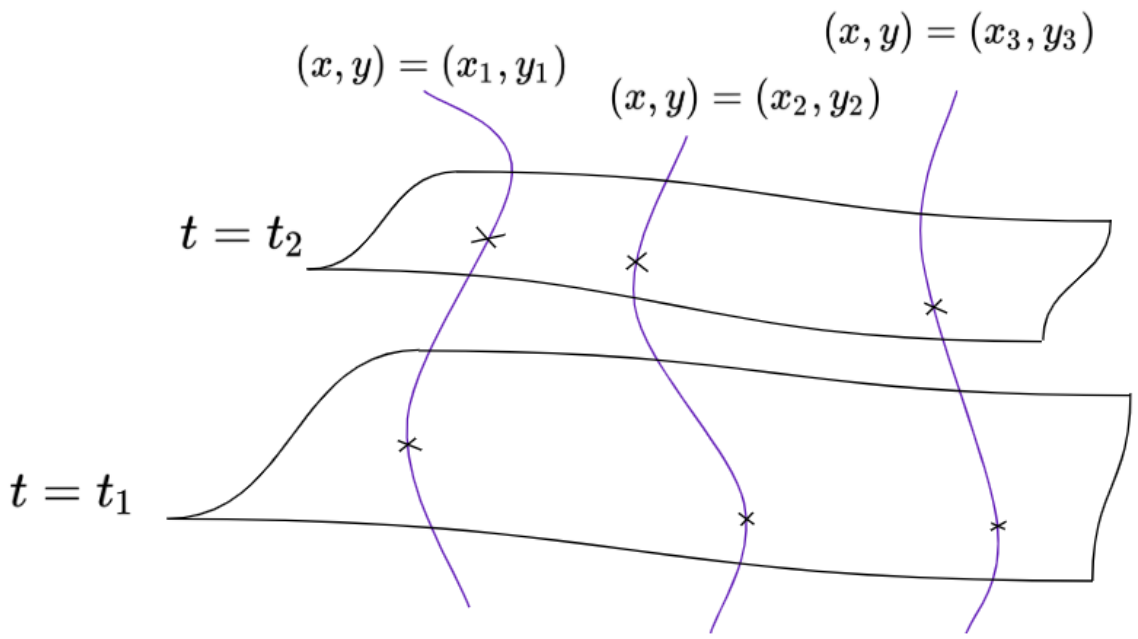

Figure 3.1: Slicing and threading of the space-time with two spacial dimensions and one time dimension. The equal time surfaces are 'pierced' by the purple threads that show equal space lines.

From this, we calculate the way the perturbed energy momentum tensor looks like after inflation

$$T_0^0 = -(\bar{\rho} + \delta\rho) \tag{3.13}$$
$$T_i^0 = (\bar{\rho} + \bar{p})av_i \tag{3.14}$$
$$T_0^i = -(\bar{\rho} + \bar{p})\frac{v^i - B^i}{a} \tag{3.15}$$
$$T_j^i = \delta_j^i(\bar{\rho} + \delta p) + \Sigma_j^i. \tag{3.16}$$

3.2 Gauge choices and transformations

We can look at different gauge choices the following way. Think of the choice of coordinates as the slicing and threading of space-time: Slicing the space time is the choosing of hypersurfaces on which all the observers have synchronised their clocks (equal time hypersurfaces), this fixes the time coordinate. Threading the space-time then corresponds to the choosing of space coordinates, on each hypersurface there is one point with a certain coordinate (see figure 3.1). Different ways of slicing the space-time corresponds to different gauge choices. With this, we can perform the ADM decomposition of the metric

$$ds^2 = -N^2dt^2 + g_{ij}\left(dx^i + N^i dt\right)\left(dx^j + N^j dt\right) \tag{3.17}$$

where N is called the lapse function and N^i is called the shift vector. We can now go from one equal time hypersurface to the next by use of these functions. This is pictured in figure 3.2.

When we have a theory without perturbations, it is easy to come up with the best way to define the slicing and threading of space-time. The threading will be defined by comoving

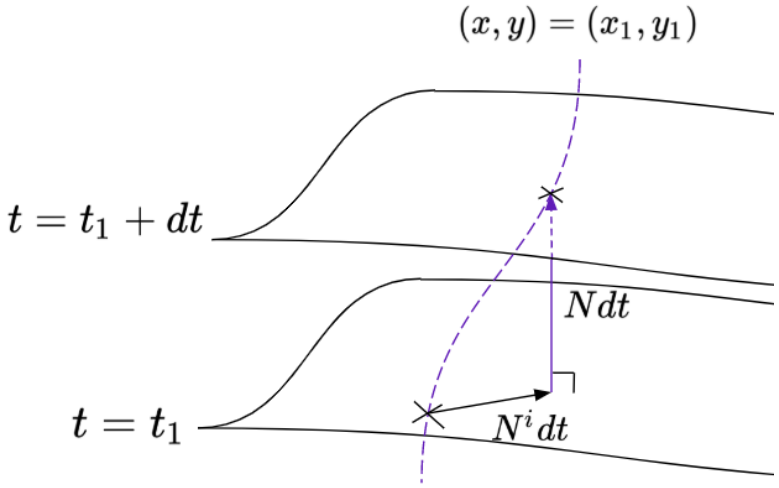

Figure 3.2: Going from one equal time hypersurface to the next while keeping the same space-coordinates by the lapse function and shift vector.

observers who see zero momentum density at their position. These free-falling observers will then observe the universe as expanding isotropically. We can then define the slicing as perpendicular to the threading, and thus make sure that the observers see the universe as homogeneous. When we have this description, we will never need a different one for a universe without perturbations. With perturbations, it is another story, but the slicing and threading will still need to reduce to the one defined before in the limit that the perturbations go to zero.

If there are perturbations present, we can always choose a slicing such that the perturbations of a certain field vanish everywhere. How can we then make sure we are looking at something physical?

We can make up a way to go from one gauge to the other. If we define a certain slicing, we can define some perturbations on that slicing, let us define these

$$\delta\phi(t, \vec{x}) = \phi(t, \vec{x}) - \bar{\phi}(x). \tag{3.18}$$

Now consider a different slicing, on which the time parameter is given by $\tilde{t}(t, \vec{x}) = \delta t(t, \vec{x}) + t$ (see figure 3.3), and define the perturbations on this slicing as

$$\delta\tilde{\phi}(\tilde{t}, \vec{x}) = \tilde{\phi}(\tilde{t}, \vec{x}) - \bar{\tilde{\phi}}(\tilde{t}). \tag{3.19}$$

We can now express (to first order) the time parameter of one slicing in terms of the other as follows

$$\tilde{t}(t - \delta t(t, \vec{x}), \vec{x}) = \tilde{t}(t, \vec{x}) - \frac{d\tilde{t}}{dt}\delta t(t, \vec{x}). \tag{3.20}$$

If we take the numerical value to be the same on both slices (which we can do without loss of generality) and put these two equations together we can conclude

$$\tilde{\delta\phi}(t, \vec{x}) = \delta\phi(t, \vec{x}) - \dot{\phi}(t)\delta t(t, \vec{x}). \tag{3.21}$$

This means that the perturbation in a scalar field does not depend on the threading.

There are some methods of slicing that are often used, so let us introduce two of them.

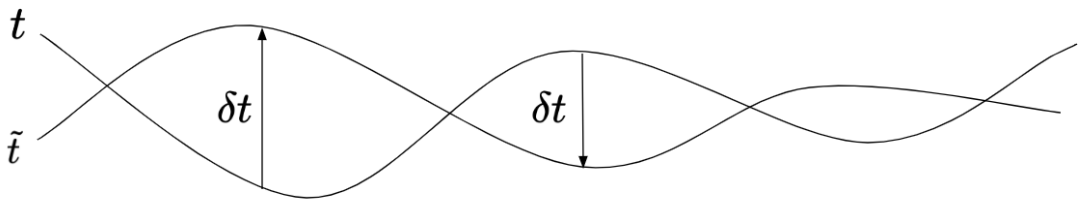

Figure 3.3: Two different ways of slicing (or defining coordinates). We take the time displacement of first order in the perturbations, and thus the time displacement is the same in both coordinates: δt.

The *comoving gauge* is defined by slicing orthogonal to comoving observers. In this gauge the perturbations in the inflaton field vanish, so $\delta\phi = 0$.

To not let the inflaton perturbations vanish, we can use the *spatially flat gauge*. In this gauge the perturbations in the metric vanish, so $Tr[g_{ij}] = 0$.

Now lets investigate how scalar and tensor perturbations act under a gauge transformation. Lets look at a gravitational gauge transformation,

$$x^\mu \to \tilde{x}^\mu = x^\mu + \xi^\mu(x), \tag{3.22}$$

where $\xi^\mu(x)$ is an arbitrary infinitesimal vector function. We know how a field and a tensor change under such a transformation

$$\phi(x) \to \tilde{\phi}(\tilde{x}) = \phi(x) \tag{3.23}$$

$$g_{\mu\nu}(x) \to \tilde{g}^{\mu\nu}(\tilde{x}) = \frac{\partial x^\rho}{\partial \tilde{x}^\mu}\frac{\partial x^\sigma}{\partial \tilde{x}^\nu} g_{\rho\sigma}(x) \tag{3.24}$$

Neglecting terms of higher order in ξ, we can rewrite this

$$\tilde{\phi}(\tau, \vec{x}) = \phi(\tau, \vec{x}) - \xi^\mu \partial_\mu \phi(\tau, \vec{x}) \tag{3.25}$$

$$\tilde{g}_{\mu\nu}(\tilde{\tau}, \tilde{\vec{x}}) = g_{\mu\nu}(\tau, \vec{x}) - \nabla_\mu \xi_\nu(\tau, \vec{x}) - \nabla_\nu \xi_\mu(\tau, \vec{x}), \tag{3.26}$$

where ∇_μ is the conformal derivative. So for our scalar perturbation we have

$$\delta\phi(\tau, \vec{x}) \to \tilde{\delta\phi}(\tau, \vec{x}) = \delta\phi(\tau, \vec{x}) - \xi^0 \partial_0 \bar{\phi}(\tau), \tag{3.27}$$

and for the tensor perturbations on the metric

$$\delta g_{\mu\nu}(x) \to \delta\tilde{g}_{\mu\nu}(\tilde{\tau}, \tilde{\vec{x}}) = \delta g_{\mu\nu}(\tau, \vec{x}) - \nabla_\mu \xi_\nu(\tau, \vec{x}) - \nabla_\nu \xi_\mu(\tau, \vec{x}). \tag{3.28}$$

We can now see that what we mean with a gauge transformation in cosmology, is actually a change of coordinate system, unlike a gauge symmetry in the Standard Model. The gauge parameter $\xi_\mu(x)$ characterizes this gauge transformation. In this case, this vector gives rise to 4 degrees of freedom, on which the perturbations are dependent. To circumvent this problem, we can either fix a gauge or only look at gauge independent quantities.

Now let us define some gauge independent quantities, which are combinations of the metric and matter perturbations. One of the most used scalar gauge invariant quantities is the curvature perturbation on uniform-density hypersurfaces, which measures the spatial curvature of constant-density hypersurfaces.

$$-\zeta \equiv \Psi + \frac{H}{\dot{\bar{\rho}}}\delta\rho. \tag{3.29}$$

What makes this quantity useful is that, for adiabatic matter perturbations, it remains constant outside the horizon. We can classify a matter perturbation as adiabatic when it obeys

$$\delta p + \frac{\dot{\bar{p}}}{\dot{\bar{\rho}}}\delta\rho = 0, \tag{3.30}$$

notice that this is a gauge invariant quantity. For single field models, the following equation is always obeyed,

$$\frac{\delta\rho_{\rm m}}{\rho_{\rm m}} = \frac{3}{4}\frac{\delta\rho_{\rm r}}{\rho_{\rm r}}, \tag{3.31}$$

which means ζ is adiabatic and does not evolve after it exits the horizon, $k \ll aH$. During SR, we can also write

$$-\zeta \approx \Psi + \frac{H}{\dot{\phi}}\delta\phi. \tag{3.32}$$

Another popular gauge invariant quantity is the comoving curvature perturbation, which measures the spatial curvature of the comoving hypersurfaces (where $\phi =$ constant),

$$\mathcal{R} \equiv \Psi - \frac{H}{\bar{\rho}+\bar{p}}\delta q \tag{3.33}$$

where δq is the scalar part of the 3-momentum density $T^0_i = \partial_i \delta q$. During inflation, we can express this in terms of the inflaton field $T^0_i = -\dot{\bar{\phi}}\partial_i\delta\phi$, which then gives

$$\mathcal{R} = \Psi + \frac{H}{\dot{\phi}}\delta\phi. \tag{3.34}$$

On super-horizon scales, $k \ll aH$, and during SR inflation, we have: $\zeta = \mathcal{R}$.

For our purposes, we consider small fluctuations to the inflationary trajectory in the spatially flat gauge ($\delta g = 0$). We have a scalar field, the inflaton ϕ, and split it in a background value $\bar{\phi}$ and a perturbation $\delta\phi$. Since we focus on the time of inflation, the inflaton is the dominant energy density. This system has the following action

$$S = \frac{1}{16\pi G}\int d^4x\sqrt{-g}R + \int d^4x(-\frac{1}{2}g^{\mu\nu}\partial_\mu\phi\partial_\nu\phi - V(\phi)) \tag{3.35}$$

Now we consider a spatially flat gauge, where our inflaton can be split in a background value, ϕ_0, and fluctuations, $\delta\phi$. We now have (this was derived by Mukhanov, and appears in the review article [24]):

$$S = \int \mathcal{L}d\tau d^3x \tag{3.36}$$

$$= \frac{1}{2}\int (v'^2 + v\Delta v + \frac{z''}{z}v^2)d\tau d^3x \tag{3.37}$$

where $v' = \partial_\tau v$, $d\tau = \frac{dt}{a}$, $v = a\delta\phi$, $z = \frac{a\phi_0'}{\mathcal{H}}$ and $\Delta = \sum_i \partial_i^2$, this is called the Mukhanov-Sasaki equation. When we vary this action with respect to v we get the following equation of motion

$$(\partial_\tau^2 - \Delta - \frac{z''}{z})v(\tau,\vec{x}) = 0. \tag{3.38}$$

Now we quantize this equation by promoting the field v and its conjugate momentum v' to quantum operators,

$$[\hat{v}(\tau,\vec{x}), \partial_\tau\hat{v}(\tau,\vec{x}')] = i\hbar\delta^3(\vec{x}-\vec{x}') \tag{3.39}$$

and move to k-space by performing a Fourier transformation,

$$\hat{v}(\tau,\vec{x}) = \int \frac{d^3k}{(2\pi)^3} e^{i\vec{k}\cdot\vec{x}}(v(\tau,k)\hat{a}(\vec{k}) + v^*(\tau,k)\hat{a}^\dagger(-\vec{k})) \tag{3.40}$$

$$(\partial_\tau^2 + k^2 - \frac{z''}{z})v(\tau,k) = 0 \tag{3.41}$$

where $k = |\vec{k}|$. Our operators $\hat{a}$ and $\hat{a}^\dagger$ obey

$$[\hat{a}(\vec{k}), \hat{a}^\dagger(\vec{k}')] = (2\pi)^3\delta^3(\vec{k} - \vec{k}'), \tag{3.42}$$

and therefore our fields $v(\tau,k)$ and $v^*(\tau,k)$ satisfy the Wronskian,

$$v(\tau,k)v^{*\prime}(\tau,k) - v^*(\tau,k)v'(\tau,k) = i. \tag{3.43}$$

The solution to the differential equation called the Bessel equation

$$x^2y'' + xy' + (b^2x^2 - n^2)y = 0 \tag{3.44}$$

where b is some constant, can be written in terms of the Hankel Functions

$$y = c_1H_n^{(1)}(ax) + c_2H_n^{(2)}(ax), \tag{3.45}$$

with c_1 and c_2 some constants. So if we can bring our equation in this form, we know the solution. Now by substituting $v = \tau^{1/2}s$ into our equation of motion and multiplying by $\tau^{3/2}$, we get

$$(\tau^2\partial_\tau^2 + \tau\partial_\tau + (k^2\tau^2 - \nu^2))s = 0 \tag{3.46}$$

$$\text{with} \quad \frac{z''}{z} = \frac{\nu^2 - \frac{1}{4}}{\tau^2}. \tag{3.47}$$

We then see that the solution is given by

$$v(\tau) = \tau^{1/2}[c_1(k)H_\nu^{(1)}(k\tau) + c_2(k)H_\nu^{(2)}(k\tau)], \tag{3.48}$$

with c_1 and c_2 some complex functions of k. v is a gauge invariant variable, defined as

$$v(k,\tau) = a(\delta\phi + \sqrt{2\epsilon}M_p\Psi). \tag{3.49}$$

In the comoving gauge $\delta\phi = 0$ this reduces to

$$v(k,\tau) = a\sqrt{2\epsilon}\Psi, \tag{3.50}$$

and in the spatially flat gauge $\delta\Psi = 0$,

$$v(k,\tau) = a\delta\phi. \tag{3.51}$$

We need the modes to change adiabatically during the matching for this method to work. In the UV the Hankel functions go as $\propto e^{-ik\tau - \frac{\pi\nu}{4}}$. The rate of change of the phase of the mode functions is then $d\Phi = ikd\tau - \frac{\pi}{4}d\nu$, this means that for them to change adiabatically, $kd\tau \gg \frac{\pi}{4}d\nu$ needs to be true. This can be put as follows

$$|k| \gg |\frac{d\nu}{d\tau}| = \mathcal{H}\partial_N\nu. \tag{3.52}$$

In the IR regime the Hankel functions go with $\propto (-k\tau)^{-\nu} = e^{-\nu\ln(-k\tau)}$. The rate of change in the mode functions is then given by $d\Phi = d\nu + \nu d\ln(-k\tau) = d\nu + \nu\frac{d\tau}{\tau}$. This boils down to the condition for adiabatic matching for IR modes:

$$\frac{d\nu}{\nu} \ll \frac{\frac{d\tau}{\tau}}{\ln(-k\tau)}, \tag{3.53}$$

or

$$\frac{d\nu}{d\tau} \ll \frac{\nu/\tau}{\ln(-k\tau)}. \tag{3.54}$$

3.3 Statistics

The quantities that are mostly studied are the power spectra of the gauge invariant quantities. These are the ones that can be observed and therefore give falsifiable predictions. The power spectrum of $\mathcal{R}$ is given by

$$\langle \mathcal{R}_{\mathbf{k}} \mathcal{R}_{\mathbf{k}'} \rangle = (2\pi)^3 \delta \left(\mathbf{k} + \mathbf{k}' \right) P_{\mathcal{R}}(k) \tag{3.55}$$

where $\langle \dots \rangle$ defines the ensemble average of the fluctuations. The dimensionless power spectrum is then given by

$$\Delta^2_{\mathcal{R}} = \frac{k^3}{2\pi^2} P_{\mathcal{R}}(k) \tag{3.56}$$

The scale dependence is also called the scalar spectral index, and defined as

$$n_s - 1 = \frac{\ln(\Delta^2_{\mathcal{R}})}{\ln(k)} \tag{3.57}$$

In the spatially flat gauge, $\mathcal{R} = \frac{\delta\phi}{\sqrt{2\epsilon}}$ so we can write

$$\Delta^2_{\mathcal{R}} = \frac{1}{2\epsilon M_P} \Delta^2_{\phi} \tag{3.58}$$

where

$$M_P^2 \equiv \frac{1}{8\pi G}. \tag{3.59}$$

From these equations it is clear that the curvature power spectrum grows as ϵ decays. During SR, ϵ stays almost constant. If there would be a scenario possible where ϵ exponentially decays, this would result in a rapid growth of the peaks in the primordial power spectrum. This is exactly what happens during a period of ultra-slow-roll, which is why we are interested in exploring what exactly will happen during such a regime.

Chapter 4

Matching

The main goal of this thesis is to continuously match the Slow-Roll perturbations to their Ultra-Slow-Roll counterpart. This is done in a couple of steps: First, we define what we mean by our switch from SR to USR. This we will do by matching the SR parameters, and showing the conditions on the modes for adiabatic matching. Then, we must make sure that there are no discontinuities in the background, as the universe cannot suddenly change. This we will do by matching the scale factor smoothly between SR and USR. Next, with this knowledge, we can match the mode functions, by calculating the Bogoliubov coefficients. Finally, we will look at the power spectra of the curvature perturbations to see how they grow during USR.

4.1 Manner of matching

As we have established, during USR the first slow-roll parameter can quickly decay. In our approximation, we take this first slow-roll parameter to be constant during slow-roll, ϵ_0,

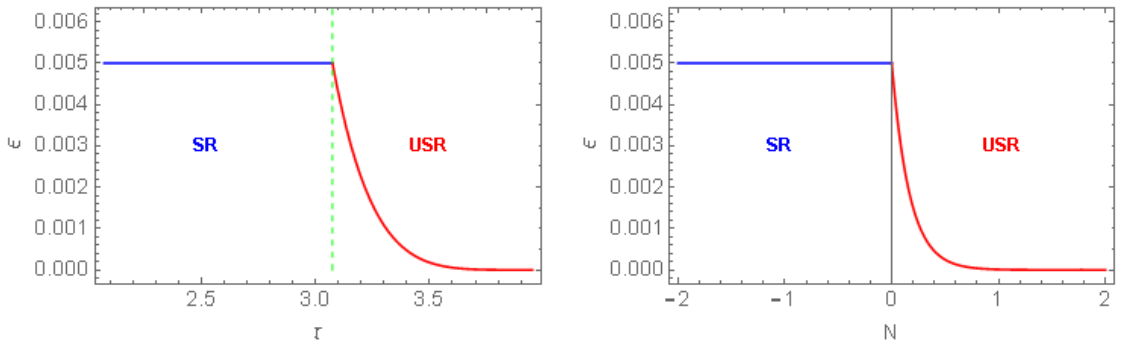

(a) The first slow-roll parameter as a function of the conformal time τ.

(b) The first slow-roll parameter as a function of the number of e-foldings N.

Figure 4.1: The first slow-roll parameter as a function of different time variables. The green line shows the time of matching, with the slow-roll regime on the left side, and the ultra-slow-roll on the right.

and to be given by,

$$\begin{aligned}\epsilon_{\rm USR} &= -\partial_N \ln(H_{\rm USR}) = -\frac{\partial_N H_{\rm USR}}{H_{\rm USR}} \\ &= -\frac{-H_0\epsilon_0 e^{-6N}}{\sqrt{\frac{\epsilon_0}{3}e^{-6N}+(1-\frac{\epsilon_0}{3})}}\frac{1}{H_0\sqrt{\frac{\epsilon_0}{3}e^{-6N}+(1-\frac{\epsilon_0}{3})}} \\ &= \frac{\epsilon_0}{\frac{\epsilon_0}{3}+(1-\frac{\epsilon_0}{3})e^{6N}},\end{aligned} \tag{4.1}$$

during ultra-slow-roll. Here we took the geometric definition of the parameter in terms of the Hubble parameter. We see, that for large N, ϵ shrinks rapidly, with $\propto e^{-6N}$. In all our plots, we took $\epsilon_0 = \frac{1}{200}$. In figure 4.1, the time dependence of ϵ is shown. We observe that the matching is continuous, but not smooth.
The second slow-roll parameter is indeed given by

$$\begin{aligned}\epsilon_2 =& \partial_N \ln(\epsilon_1) \\ =& -6 + 2\frac{\epsilon_0}{\frac{\epsilon_0}{3}-(\frac{\epsilon_0}{2}-1)e^{6N}} \\ =& -6 + 2\epsilon_1\end{aligned} \tag{4.2}$$

4.2 Background

We will match the scale factor in SR to the scale factor in USR, and do the same with the Hubble parameter. We have some freedom in choosing the time shift, so we can choose to do the matching of a and H at $\hat{N} = 0$. From now on, a hat will show the value is taken at the time of matching. With this choice, in Ultra Slow-Roll we have,

$$\hat{a}_{\rm USR}(N) = a_0 e^{\hat{N}} = a_0. \tag{4.3}$$

Now we want to match this smoothly to its Slow-Roll counterpart. To make sure the scale factor is neatly matched, we put

$$\begin{aligned}\hat{a}_{\rm USR} &= \hat{a}_{\rm SR} \\ a_0 e^{\hat{N}} &= a_0(1-(1-\epsilon_0)a_0 H_0(\hat{\tau}-\tau_0))^{-\frac{1}{1-\epsilon_0}} \\ a_0 &= a_0(1-(1-\epsilon_0)a_0 H_0(\hat{\tau}-\tau_0))^{-\frac{1}{1-\epsilon_0}} \\ \Rightarrow \tau_0 &= \hat{\tau}.\end{aligned} \tag{4.4}$$

Now the scale factor is matched, but we should still make sure this is smoothly done. We can match a' for this purpose, but as $\mathcal{H} = \frac{a'}{a}$ and we know a is already matched, we can also choose to match $\mathcal{H}_{\rm SR}$ and $\mathcal{H}_{\rm USR}$ at $\tau = \hat{\tau}$. The expression for the Hubble parameter in Ultra Slow-Roll is

$$H_{\rm USR}(N) = H_0\sqrt{\frac{\epsilon_0}{3}e^{-6N}+1-\frac{\epsilon_0}{3}} \tag{4.5}$$

$$\hat{H}_{\rm USR} = H_0. \tag{4.6}$$

Now we have for the Hubble parameter (in conformal time) in USR,

$$\mathcal{H}_{\rm USR}(N) = a_0 e^N H_0\sqrt{\frac{\epsilon_0}{3}e^{-6N}+1-\frac{\epsilon_0}{3}} \tag{4.7}$$

$$\hat{\mathcal{H}}_{\rm USR} = a_0 H_0 = \mathcal{H}_0. \tag{4.8}$$

For the Hubble parameter in SR we have

$$\mathcal{H}_{\rm SR} = a_0 H_0 (1 - (1-\epsilon_0) a_0 H_0 (\tau - \tau_0))^{-1}. \tag{4.9}$$

Now matching these gives

$$\begin{aligned} \hat{\mathcal{H}}_{\rm USR} &= \hat{\mathcal{H}}_{\rm SR} \\ a_0 H_0 &= a_0 H_0 (1 - (1-\epsilon_0) a_0 H_0 (\hat{\tau} - \tau_0))^{-1} \\ \Rightarrow \tau_0 &= \hat{\tau}. \end{aligned} \tag{4.10}$$

So we finally have

$$a_{\rm SR}(\tau) = a_0 (1 - (1-\epsilon_0) a_0 H_0 (\tau - \hat{\tau}))^{-\frac{1}{1-\epsilon_0}} \tag{4.11}$$

$$a_{\rm USR}(N) = a_0 e^N \tag{4.12}$$

$$\mathcal{H}_{\rm SR}(\tau) = a_0 H_0 (1 - (1-\epsilon_0) a_0 H_0 (\tau - \hat{\tau}))^{-1} \tag{4.13}$$

$$\mathcal{H}_{\rm USR}(N) = a_0 e^N H_0 \sqrt{\frac{\epsilon_0}{3} e^{-6N} + 1 - \frac{\epsilon_0}{3}}. \tag{4.14}$$

To compare these, we need to express the Ultra-Slow-Roll quantities in τ just like the Slow-Roll ones. So we need to find an expression for N or $a = e^N$ in terms of τ.
We know that the conformal time since the matching point is given by

$$\begin{aligned} \tau(N^*) &= \int_0^{N^*} \frac{dN}{aH} \\ &= \int_0^{N^*} \frac{e^{-N} dN}{a_0 H_0 \sqrt{(\epsilon_0/3) e^{-6N} + (1 - \epsilon_0/3)}}. \end{aligned} \tag{4.15}$$

Here τ is the conformal time since the time of matching. To get just the conformal time, we need to add the conformal time at the time of matching ($\hat{\tau}$) to the right hand side of the equation. We can substitute the following

$$\begin{aligned} x &= (3/\epsilon_0 - 1)^{1/3} e^{2N} \\ dN = \frac{dx}{2x}, \quad e^{6N} &= \frac{x^3}{(\frac{3}{\epsilon_0} - 1)^1}, \end{aligned}$$

so the integral becomes:

$$\tau(N^*) = \frac{(\frac{3}{\epsilon_0} - 1)^{1/6}}{2 a_0 H_0 \sqrt{1 - \frac{\epsilon_0}{3}}} \int_{(3/\epsilon_0 - 1)^{1/3}}^{(3/\epsilon_0 - 1)^{1/3} e^{2N^*}} \frac{dx}{\sqrt{1 + x^3}} \tag{4.16}$$

which we need to invert. To do this, we first split it

$$\begin{aligned} \tau(N^*) &= \frac{(\frac{3}{\epsilon_0} - 1)^{1/6}}{2 a_0 H_0 \sqrt{1 - \frac{\epsilon_0}{3}}} \int_{(3/\epsilon_0 - 1)^{1/3}}^{(3/\epsilon_0 - 1)^{1/3} e^{2N^*}} \frac{dx}{\sqrt{1 + x^3}} \\ &= \frac{(\frac{3}{\epsilon_0} - 1)^{1/6}}{2 a_0 H_0 \sqrt{1 - \frac{\epsilon_0}{3}}} \left(\int_0^{(3/\epsilon_0 - 1)^{1/3} e^{2N^*}} \frac{dx}{\sqrt{1 + x^3}} - \int_0^{(3/\epsilon_0 - 1)^{1/3}} \frac{dx}{\sqrt{1 + x^3}} \right), \end{aligned} \tag{4.17}$$

then call

$$I(y) = \int_0^y \frac{dx}{\sqrt{1 + x^3}}, \tag{4.18}$$

such that

$$\tau(N^*) = \frac{(\frac{3}{\epsilon_0} - 1)^{1/6}}{2a_0 H_0 \sqrt{1 - \frac{\epsilon_0}{3}}} (I((3/\epsilon_0 - 1)^{1/3} e^{2N^*}) - I((3/\epsilon_0 - 1)^{1/3})) \tag{4.19}$$

and start with calculating $I(y)$.

We write this integral as an integral over a series

$$\begin{aligned} I(y) &= \int_0^y \sum_{n=0}^{\infty} \frac{(-1)^n x^{3n} (\frac{1}{2})_n}{n!} dx \\ &= \sum_{n=0}^{\infty} \frac{(-1)^n (\frac{1}{2})_n}{n!} \int_0^y x^{3n} dx \\ &= \sum_{n=0}^{\infty} \frac{(-1)^n (\frac{1}{2})_n}{n!} \frac{y^{3n+1}}{3n+1}, \end{aligned} \tag{4.20}$$

where

$$\begin{aligned} (a)_n &= a(a+1)(a+2)\dots(a+n-1) = \frac{(a+n-1)!}{(a-1)!} \\ &= \frac{\Gamma(a+n)}{\Gamma(a)}. \end{aligned} \tag{4.21}$$

Now we write

$$\begin{aligned} \frac{1}{3n+1} &= \frac{1}{3} \frac{1}{n+1/3} \\ &= \frac{1}{3} \frac{\Gamma(1/3+n)}{\Gamma(4/3+n)} \\ &= \frac{1}{3} \frac{\Gamma(1/3+n)}{\Gamma(1/3)} \frac{\Gamma(4/3)}{\Gamma(4/3+n)} \frac{\Gamma(1/3)}{\Gamma(4/3)} \\ &= \frac{1}{3} \frac{(\frac{1}{3})_n}{(\frac{4}{3})_n} 3 \\ &= \frac{(\frac{1}{3})_n}{(\frac{4}{3})_n}. \end{aligned} \tag{4.22}$$

And finally we have

$$I(y) = y \sum_{n=0}^{\infty} \frac{(\frac{1}{2})_n (\frac{1}{3})_n}{(\frac{4}{3})_n} \frac{(-y^3)^n}{n!} \tag{4.23}$$

$$= y \, {}_2F_1\left(\frac{1}{2}, \frac{1}{3}; \frac{4}{3}; -y^3\right), \tag{4.24}$$

where ${}_2F_1(\alpha, \beta; \gamma; z)$ is the hypergeometric function

$${}_2F_1(\alpha, \beta; \gamma; z) = \sum_{n=0}^{\infty} \frac{(\alpha)_n (\beta)_n}{(\gamma)_n} \frac{z^n}{n!} \tag{4.25}$$

Now back to the original equation, we have the following (exact) expression for τ in terms of N:

$$\begin{aligned}\tau(N^*) =& \frac{(\frac{3}{\epsilon_0}-1)^{1/6}}{2a_0H_0\sqrt{1-\frac{\epsilon_0}{3}}}\left[(3/\epsilon_0-1)^{1/3}e^{2N^*}\,{}_2F_1\left(\frac{1}{2},\frac{1}{3};\frac{4}{3};-((3/\epsilon_0-1)^{1/3}e^{2N^*})^3\right)\right.\\ &\left.-(3/\epsilon_0-1)^{1/3}\,{}_2F_1\left(\frac{1}{2},\frac{1}{3};\frac{4}{3};-((3/\epsilon_0-1)^{1/3})^3\right)\right]\\ =& \frac{\sqrt{\frac{3}{\epsilon_0}}}{2a_0H_0}\left[e^{2N^*}\,{}_2F_1\left(\frac{1}{2},\frac{1}{3};\frac{4}{3};-(3/\epsilon_0-1)e^{6N^*}\right)\right.\\ &\left.-\,{}_2F_1\left(\frac{1}{2},\frac{1}{3};\frac{4}{3};-(3/\epsilon_0-1)\right)\right].\end{aligned} \tag{4.26}$$

We have set the time of matching at $N=0$, so what is calculated is the conformal time since the matching. This means that from this equation, the time of matching in conformal time τ can be read off. Now there are two options: $\tau(\hat{N})$ can be put to zero, then the value of $\Delta\tau$ can be read off from this equation,

$$\Delta\tau = \frac{1}{2a_0H_0\sqrt{\epsilon_0/3}}\,{}_2F_1\left(\frac{1}{2},\frac{1}{3};\frac{4}{3};-(3/\epsilon_0-1)\right). \tag{4.27}$$

Alternatively, we can perform some shift in time, such that $\Delta\tau$ vanishes. This way

$$\hat{\tau} = \tau(\hat{N}) = \tau(0) = \frac{1}{2a_0H_0\sqrt{\epsilon_0/3}}\,{}_2F_1\left(\frac{1}{2},\frac{1}{3};\frac{4}{3};-(3/\epsilon_0-1)\right). \tag{4.28}$$

Both of these equations can, however, be written in the following way

$$\tau+\Delta\tau = \frac{1}{2a_0H_0\sqrt{\frac{\epsilon_0}{3}}}e^{2N^*}\,{}_2F_1\left(\frac{1}{2},\frac{1}{3};\frac{4}{3};-(3/\epsilon_0-1)e^{6N^*}\right). \tag{4.29}$$

This equation cannot be analytically inverted, so we have to look at different limits. Let's start with the limit for large N. From Table of Integrals, Series, and Products [25] we know the following relation to be true (when $|arg(z)|<\pi$ and $\alpha-\beta\neq m$ where $m=0,1,2,\dots$):

$$\begin{aligned}F(\alpha,\beta;\gamma;z) =& \frac{\Gamma(\gamma)\Gamma(\beta-\alpha)}{\Gamma(\beta)\Gamma(\gamma-\alpha)}(-z)^{-\alpha}F\left(\alpha,\alpha+1-\gamma;\alpha+1-\beta;\frac{1}{z}\right)\\ &+\frac{\Gamma(\gamma)\Gamma(\alpha-\beta)}{\Gamma(\alpha)\Gamma(\gamma-\beta)}(-z)^{-\beta}F\left(\beta,\beta+1-\gamma;\beta+1-\alpha;\frac{1}{z}\right).\end{aligned} \tag{4.30}$$

This means we can rewrite our equation 4.29

$$
\begin{aligned}
2a_0H_0\sqrt{\frac{\epsilon_0}{3}}(\tau+\Delta\tau) = e^{2N^*}\Bigg[& \\
& \frac{\Gamma(\frac{4}{3})\Gamma(\frac{-1}{6})}{\Gamma(\frac{1}{3})\Gamma(\frac{5}{6})}(3/\epsilon_0-1)^{-1/2}e^{-3N^*}\,{}_2F_1\left(\frac{1}{2},\frac{1}{6};\frac{7}{6};\frac{-1}{(3/\epsilon_0-1)e^{6N^*}}\right) \\
& +\frac{\Gamma(\frac{4}{3})\Gamma(\frac{1}{6})}{\Gamma(\frac{1}{2})\Gamma(1)}(3/\epsilon_0-1)^{-1/3}e^{-2N^*}\,{}_2F_1\left(\frac{1}{3},0;\frac{5}{6};\frac{-1}{(3/\epsilon_0-1)e^{6N^*}}\right)\Bigg] \\
= e^{2N^*}\Bigg[& \\
& -2(3/\epsilon_0-1)^{-1/2}e^{-3N^*}\,{}_2F_1\left(\frac{1}{2},\frac{1}{6};\frac{7}{6};\frac{-1}{(3/\epsilon_0-1)e^{6N^*}}\right) \\
& +\frac{\Gamma(\frac{4}{3})\Gamma(\frac{1}{6})}{\sqrt{\pi}}(3/\epsilon_0-1)^{-1/3}e^{-2N^*}\Bigg].
\end{aligned}
\tag{4.31}
$$

We can perform a Taylor expansion for large N, that is around $e^{-N}=0$, of the hypergeometric function in this expression. Doing this, we find op to order $\mathcal{O}(e^{-18N^*})$

$$
2a_0H_0\sqrt{\frac{\epsilon_0}{3}}(\tau+\Delta\tau) = e^{2N^*} \tag{4.32}
$$

$$
\begin{aligned}
\Bigg[-2(\frac{3}{\epsilon_0}-1)^{-1/2}e^{-3N^*}(1+\frac{1}{14}(\frac{-1}{\frac{3}{\epsilon_0}-1})e^{-6N^*}+\frac{3}{104}(\frac{1}{\frac{3}{\epsilon_0}-1})^2e^{-12N}+\mathcal{O}(e^{-18N^*})) & \\
+\frac{\Gamma(\frac{4}{3})\Gamma(\frac{1}{6})}{\sqrt{\pi}}(\frac{3}{\epsilon_0}-1)^{-1/3}e^{-2N^*} & \\
= -2(\frac{3}{\epsilon_0}-1)^{-1/2}e^{-N^*}(1+\frac{1}{14}(\frac{-1}{\frac{3}{\epsilon_0}-1})e^{-6N^*}+\frac{3}{104}(\frac{1}{\frac{3}{\epsilon_0}-1})^2e^{-12N}+\mathcal{O}(e^{-18N^*})) & \\
+\frac{\Gamma(\frac{4}{3})\Gamma(\frac{1}{6})}{\sqrt{\pi}}(\frac{3}{\epsilon_0}-1)^{-1/3} &
\end{aligned}
\tag{4.33}
$$

This means, that for large enough N, e^{-N} can be approximated by

$$
\begin{aligned}
e^{-N} &= -\big[a_0H_0\sqrt{\frac{\epsilon_0}{3}}(\tau+\Delta\tau)-\frac{\Gamma(\frac{4}{3})\Gamma(\frac{1}{6})}{2\sqrt{\pi}}(\frac{3}{\epsilon_0}-1)^{-1/3}\big](\frac{3}{\epsilon_0}-1)^{1/2} \\
&= -a_0H_0\sqrt{1-\frac{\epsilon_0}{3}}(\tau+\Delta\tau)+\frac{\Gamma(\frac{4}{3})\Gamma(\frac{1}{6})}{2\sqrt{\pi}}(\frac{3}{\epsilon_0}-1)^{1/6},
\end{aligned}
\tag{4.34}
$$

or

$$
a = a_0e^N = \frac{1}{-H_0\sqrt{1-\frac{\epsilon_0}{3}}(\tau+\Delta\tau)}(1+\frac{1}{14}(\frac{-1}{3/\epsilon_0-1})e^{-6N}+\frac{3}{104}(\frac{1}{\frac{3}{\epsilon_0}-1})^2e^{-12N}+\mathcal{O}(e^{-18N^*})), \tag{4.35}
$$

where we absorb the constant factor in $\Delta\tau$ which now reads

$$
\Delta\tau = -\frac{\Gamma(\frac{4}{3})\Gamma(\frac{1}{6})}{2a_0H_0\sqrt{1-\frac{\epsilon_0}{3}}\sqrt{\pi}}(\frac{3}{\epsilon_0}-1)^{1/6} \tag{4.36}
$$

As we know, this should be equal to a_0 when $N=0$. With this approximation, we can

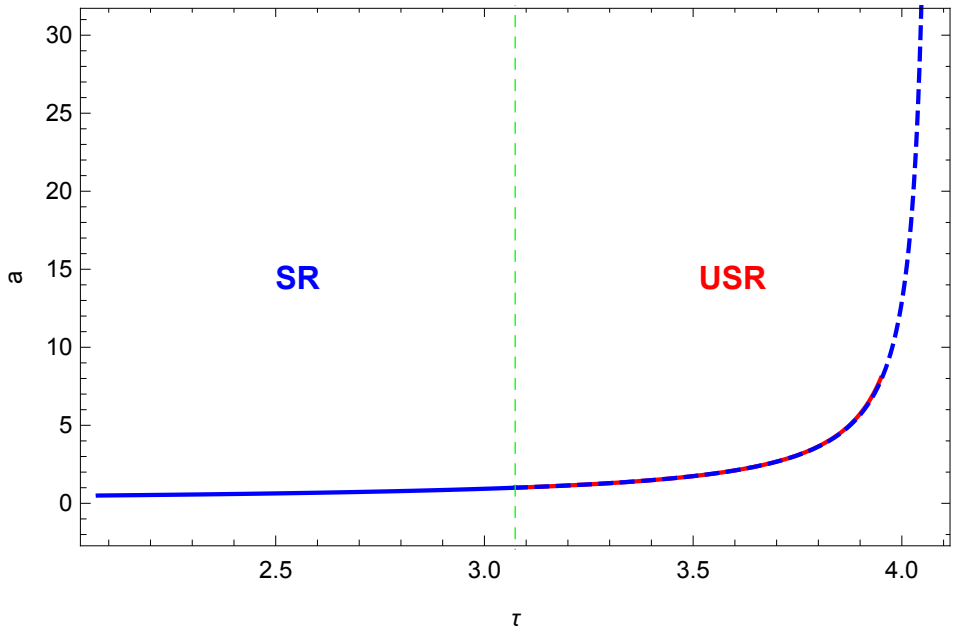

Figure 4.2: The matched scale factor with $\epsilon_0 = \frac{1}{200}$, $k = 0.1$, $a_0 = 1$ and $\mathcal{H}_0 = 1$. The blue line correspond to the scale factor in the slow-roll regime and the red to the scale factor in the ultra-slow-roll regime. The blue dotted line is the evolution that the scale factor would undergo if the SR approximation did not fail.

also find an approximated version of $\mathcal{H}_{\text{USR}}(\tau)$,

$$\begin{aligned}\mathcal{H} = aH =& a_0 e^N H_0 \sqrt{\frac{\epsilon_0}{3} e^{-6N} + 1 - \frac{\epsilon_0}{3}} \\ =& \frac{1}{-\sqrt{1-\frac{\epsilon_0}{3}}(\tau + \Delta\tau)} (1 + \frac{1}{14}(\frac{-1}{\frac{3}{\epsilon_0} - 1}) e^{-6N} + \frac{3}{104}(\frac{1}{\frac{3}{\epsilon_0} - 1})^2 e^{-12N} + \mathcal{O}(e^{-18N^*})) \\ & \times \sqrt{\frac{\epsilon_0}{3} e^{-6N} + 1 - \frac{\epsilon_0}{3}} \\ =& \frac{1}{-(\tau + \Delta\tau)} (1 + \frac{1}{14}(\frac{-1}{\frac{3}{\epsilon_0} - 1}) e^{-6N} + \frac{3}{104}(\frac{1}{\frac{3}{\epsilon_0} - 1})^2 e^{-12N} + \mathcal{O}(e^{-18N^*})) \\ & \times \sqrt{1 + \frac{1}{\frac{3}{\epsilon_0} - 1} e^{-6N}}. \end{aligned} \tag{4.37}$$

In figure 4.2, were we plotted the exact expression for the scale factor (from the inverse function of τ), it is shown that the continued SR scale factor does not differ much from the USR scale factor. This is to be expected, as they are depended on τ, $\mathcal{H}_0$ and ϵ, and only ϵ changes after the matching. Since ϵ is continuous at the matching, we see only a slight difference in the evolution of the scale factor. The same can be seen in figure 4.3, where we plotted the Hubble parameter before and after the matching.

4.3 Mode Functions

4.3.1 Small detour to calculate ν

To see the behaviour of ν during USR we need to put the expressions for ϵ_1 and $\mathcal{H}$ in terms of τ with corrections of order e^{-6N} in the equation of motion (eq.3.46). We can start with calculating $\frac{z''}{z}$ in terms of τ with corrections of e^{-6N}. To do this we have used

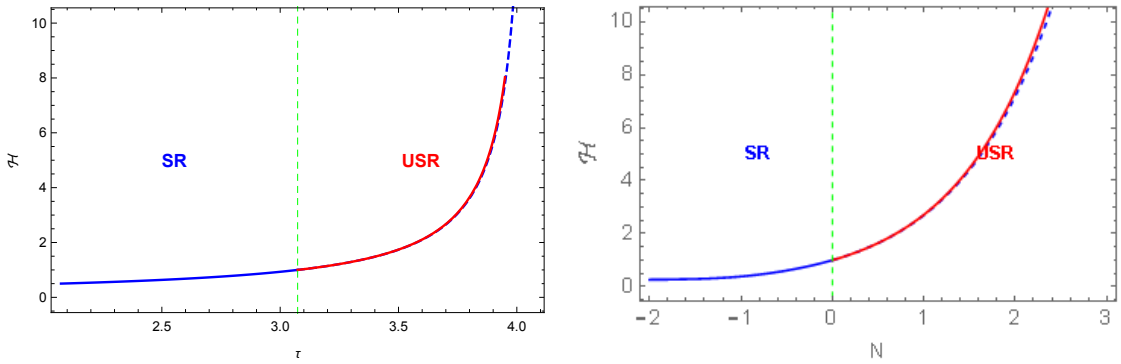

(a) The matched Hubble parameter with $\epsilon_0 = \frac{1}{200}$, $k = 0.1$, $a_0 = 1$ and $\mathcal{H}_0 = 1$

(b) The matched Hubble parameter with $\epsilon_0 = \frac{1}{200}$, $k = 0.1$, $a_0 = 1$ and $\mathcal{H}_0 = 1$

Figure 4.3: The matched Hubble parameter with $\epsilon_0 = \frac{1}{200}$, $k = 0.1$, $a_0 = 1$ and $\mathcal{H}_0 = 1$ The green line shows the time of matching, with the slow-roll regime on the left side, and the ultra-slow-roll on the right. The blue line correspond to the conformal Hubble parameter in the slow-roll regime and the red to the conformal Hubble parameter in the ultra-slow-roll regime. The blue dotted line is the evolution that the conformal Hubble parameter would undergo if the SR approximation did not fail.

the expressions $\epsilon_2 = -6 + 2\epsilon_1$ and $\epsilon_3 = 2\epsilon_1$ and higher order slow-roll parameters 2.46. Now we know the expression for $\frac{z''}{z}$ in terms of the SR parameter,

$$\frac{z''}{z} = \mathcal{H}^2(2 - 7\epsilon_1 + 2\epsilon_1^2) \tag{4.38}$$

$$= \mathcal{H}^2(2 - \frac{21e^{-6N}}{e^{-6N} + \frac{3}{\epsilon_0} - 1} + \frac{18e^{-12N}}{(e^{-6N} + \frac{3}{\epsilon_0} - 1)^2}), \tag{4.39}$$

which is an exact expression. We use the expression for $\mathcal{H}^2$ that we found, with corrections in e^{-N} to get

$$\begin{aligned}\frac{z''}{z} =& \frac{1}{(\tau + \Delta\tau)^2}(1 + \frac{1}{14}(\frac{-1}{\frac{3}{\epsilon_0} - 1})e^{-6N} + \frac{3}{104}(\frac{1}{\frac{3}{\epsilon_0} - 1})^2 e^{-12N} + \mathcal{O}(e^{-18N^*}))^2 \\ & \times (1 + \frac{1}{\frac{3}{\epsilon_0} - 1}e^{-6N}) \\ & \times (2 - \frac{21}{\frac{3}{\epsilon_0} - 1}e^{-6N} + \frac{39}{(\frac{3}{\epsilon_0} - 1)^2}e^{-12N} + \mathcal{O}(e^{-18N})) \\ =& \frac{1}{(\tau + \Delta\tau)^2}(2 - \frac{135}{7}\frac{e^{-6N}}{(\frac{3}{\epsilon_0} - 1)} + \frac{13275}{637}\frac{e^{-12N}}{(\frac{3}{\epsilon_0} - 1)^2} + \mathcal{O}(e^{-18N})).\end{aligned} \tag{4.40}$$

With the expression for $\frac{z''}{z}$, we can finally calculate ν^2,

$$\nu^2_{\text{USR}} = (\tau + \Delta\tau)^2\frac{z''}{z} + \frac{1}{4} \tag{4.41}$$

$$= \frac{9}{4} - \frac{135}{7}\frac{e^{-6N}}{(\frac{3}{\epsilon_0} - 1)} + \frac{13275}{637}\frac{e^{-12N}}{(\frac{3}{\epsilon_0} - 1)^2} + \mathcal{O}(e^{-18N}). \tag{4.42}$$

$$\tag{4.43}$$

This gives for ν,

$$\begin{aligned}\nu_{\text{USR}} &= \sqrt{\frac{9}{4} - \frac{135}{7}\frac{e^{-6N}}{(\frac{3}{\epsilon_0}-1)} + \frac{13275}{637}\frac{e^{-12N}}{(\frac{3}{\epsilon_0}-1)^2} + \mathcal{O}(e^{-18N}} \\ &= \sqrt{\frac{9}{4} - \frac{135}{7}\frac{\epsilon_1}{3-\epsilon_1} + \frac{13275}{637}\frac{\epsilon_1^2}{(3-\epsilon_1)^2} + \mathcal{O}(e^{-18N}} \\ &= \frac{3}{2} + \delta\nu_{\text{USR}} \qquad (4.44)\end{aligned}$$

where

$$\delta\nu_{\text{USR}} = -\frac{15}{7}\epsilon_1 - \frac{2815}{1911}\epsilon_1^2. \qquad (4.45)$$

As can been seen in figure 4.4, there is a discontinuity in ν at the matching. This can be explained by remembering that while ϵ_1 is continuous, ϵ_2 experiences a jump, and ν is dependent on both. We do not see the dependence of ν on ϵ_2 here, because we expressed ϵ_2 in terms of ϵ_1.

We can now check the constraints for adiabatic change. In the UV, we had $kd\tau \gg d\nu$. We can find an expression for $d\tau$ from equation 4.29,

$$\begin{aligned}d\tau =& \frac{e^{2N}dN}{2a_0H_0\sqrt{\frac{\epsilon_0}{3}}}\Big(2{}_2F_1(\frac{1}{2},\frac{1}{3};\frac{4}{3};-(\frac{3}{\epsilon_0}-1)e^{6N}) + \frac{2}{\sqrt{1-(1-\frac{3}{\epsilon_0})e^{6N}}} - 2{}_2F_1(\frac{1}{2},\frac{1}{3};\frac{4}{3};-(\frac{3}{\epsilon_0}-1)e^{6N})\Big) \\ =& \frac{dN}{a_0H_0\sqrt{\frac{\epsilon_0}{3}}}\frac{e^{2N}}{\sqrt{1-(1-\frac{3}{\epsilon_0})e^{6N}}} \\ =& \frac{dN}{a_0H_0\sqrt{\frac{\epsilon_0}{3}}} \quad \text{at the time of matching.} \qquad (4.46)\end{aligned}$$

For $d\nu$ we can now find

$$\begin{aligned}d\nu \approxeq d\epsilon_1 &= -\frac{6(1-\frac{\epsilon_0}{3})\epsilon_0 e^{6N}}{((1-\frac{\epsilon_0}{3})e^{6N}+\frac{\epsilon_0}{3})^2}dN \\ &= -6(1-\frac{\epsilon_0}{3})\epsilon_0 dN \quad \text{at the time of matching.} \qquad (4.47)\end{aligned}$$

This gives the condition for adiabaticity for the UV modes

$$|k| \gg |a_0H_0\sqrt{\frac{\epsilon_0}{3}}(-6(1-\frac{\epsilon_0}{3}))|. \qquad (4.48)$$

Similarly we can find for the IR modes the condition for adiabaticity at the matching:

$$\ln(-k\hat{\tau}) \ll \frac{\nu_{\text{USR}}}{\hat{\tau}(\frac{90}{7}\epsilon_0(1-\frac{\epsilon_0}{3}))}. \qquad (4.49)$$

4.3.2 Bogoliubov coefficients

To see how fluctuations in the inflaton field change when we are in the Ultra Slow Roll (USR) regime instead of Slow Roll (SR) regime, we match the two solutions at some time $\tau = \tau_{\text{matching}} = \hat{\tau}$:

$$\begin{aligned}\phi_{\text{USR}} &= \phi_{\text{SR}} && \text{at} \tau_{\text{matching}} \\ \phi'_{\text{USR}} &= \phi'_{\text{SR}} && \text{at} \tau_{\text{matching}},\end{aligned}$$

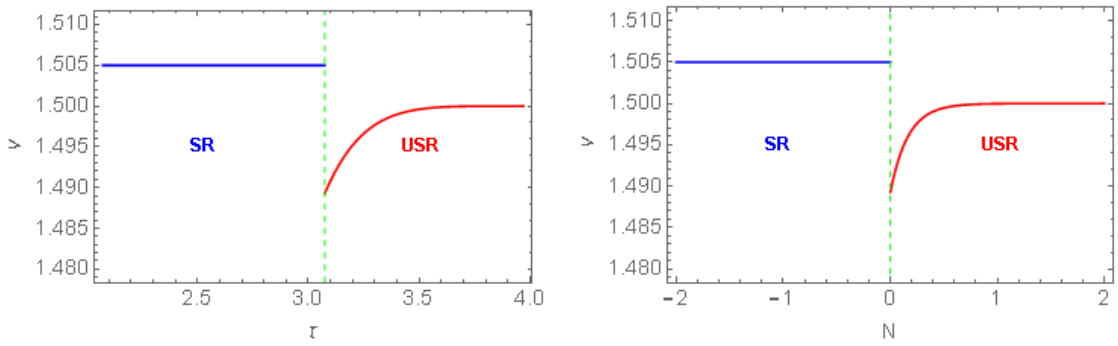

(a) ν as a function of the conformal time τ.

(b) ν as a function of the number of e-foldings N.

Figure 4.4: ν as a function of two different time variables. The green line shows the time of matching, with the slow-roll regime on the left side, and the ultra-slow-roll on the right.

where the prime denotes a derivative to τ. We write the wave equations in terms of Hankel functions in the following way:

$$\phi_{\mathrm{SR}} = \frac{1}{a}\sqrt{\frac{-\pi(\tau+\Delta\tau_{\mathrm{SR}})}{4}}H^{(2)}_{\nu_{\mathrm{SR}}}(-k(\tau+\Delta\tau_{\mathrm{SR}}) \tag{4.50}$$

$$\phi_{\mathrm{USR}} = \frac{1}{a}\sqrt{\frac{-\pi(\tau+\Delta\tau_{\mathrm{USR}})}{4}}(\alpha(k)H^{(2)}_{\nu_{\mathrm{USR}}}(-k(\tau+\Delta\tau_{\mathrm{USR}})) + \beta(k)H^{(1)}_{\nu_{\mathrm{USR}}}(-k(\tau+\Delta\tau_{\mathrm{USR}}))), \tag{4.51}$$

here, we assume that we can write the wave equation during SR in the Bunch-Davies vacuum, with only right moving modes. We can fix the $\alpha(k)$ and $\beta(k)$ with the matching procedure. We have now continuously matched $a_{\mathrm{SR}}(\tau)$ to $a_{\mathrm{USR}}(\tau)$ and $H_{\mathrm{SR}}(\tau)$ to $H_{\mathrm{USR}}(\tau)$. So now we will match the mode functions by finding expressions for $\alpha(k)$ and $\beta(k)$.

To find the expressions for the coefficients α and β we first write

$$\phi_{\mathrm{SR}} = \phi^* \tag{4.52}$$

$$\phi_{\mathrm{USR}} = \alpha\psi^* + \beta\psi \tag{4.53}$$

then we impose the matching conditions

$$\phi^* = \alpha\psi^* + \beta\psi \tag{4.54}$$

$$\phi^{*\prime} = \alpha\psi^{*\prime} + \beta\psi'. \tag{4.55}$$

We furthermore know the Wronskian:

$$\phi\phi^{*\prime} - \phi^*\phi' = \frac{i}{a^2} \tag{4.56}$$

$$|\alpha|^2 - |\beta|^2 = 1, \tag{4.57}$$

By multiplying 4.54 with $\psi^{*\prime}$ and subtracting 4.55 times ψ^* we get the following equation for β (where we used the Wronskian 4.56)

$$\phi^*\psi' - \phi^{*\prime}\psi = \beta(\psi\psi^{*\prime} - \psi'\psi^*) = -i\beta. \tag{4.58}$$

Repeating the same trick, but with ψ^* instead of ψ, we find the following equations for α and β

$$\alpha = i(\phi^*\psi' - \phi^{*\prime}\psi) \tag{4.59}$$
$$\beta = -i(\phi^*\psi^{*\prime} - \phi^{*\prime}\psi^*). \tag{4.60}$$

Now with the use of hyper geometric functions we found an expression for ν_{USR}, so we know

$$\nu_{\mathrm{SR}} = \frac{3}{2} + \epsilon_1 + \mathcal{O}(\epsilon_1^2) \tag{4.61}$$
$$\nu_{\mathrm{USR}} = \frac{3}{2} + \delta\nu_{\mathrm{USR}} \tag{4.62}$$
$$\delta\nu_{\mathrm{USR}} = -\frac{15}{7}\epsilon_1 - \frac{2815}{1911}\epsilon_1^2 + \mathcal{O}(\epsilon_1^3), \tag{4.63}$$

where we can ignore $\mathcal{O}(\epsilon_1^2)$ because this is sufficiently small at the time of matching. Notice how the expressions for ν_{USR} do not depend on the higher SR parameters. In USR these higher SR parameters are no longer independent variables, and can be expressed in terms of the first SR parameter, which is what we have done here.

Now expressions for $\alpha(k)$ and $\beta(k)$ are needed. Let us start with calculating α

$$\alpha = i(\phi^*\psi' - \phi^{*\prime}\psi) \tag{4.64}$$
$$\begin{aligned} =i\Bigg[&\sqrt{-\frac{\pi}{4}(\tau+\Delta\tau_{\mathrm{SR}})}\frac{1}{a_{\mathrm{SR}}}H^{(2)}_{\nu_{\mathrm{SR}}}(-k(\tau+\Delta\tau_{\mathrm{SR}}))\sqrt{-\frac{\pi}{4}(\tau+\Delta\tau_{\mathrm{USR}})}\partial_\tau\frac{1}{a_{\mathrm{USR}}}H^{(1)}_{\nu_{\mathrm{USR}}}(-k(\tau+\Delta\tau_{\mathrm{USR}}))\\ &+\frac{\frac{\pi}{4}(\Delta\tau_{\mathrm{USR}}-\Delta\tau_{\mathrm{SR}})}{\sqrt{(\tau+\Delta\tau_{\mathrm{SR}})(\tau+\Delta\tau_{\mathrm{USR}})}}\frac{1}{a_{\mathrm{SR}}}H^{(2)}_{\nu_{\mathrm{SR}}}(-k(\tau+\Delta\tau_{\mathrm{SR}}))\frac{1}{a_{\mathrm{USR}}}H^{(1)}_{\nu_{\mathrm{USR}}}(-k(\tau+\Delta\tau_{\mathrm{USR}}))\\ &-\sqrt{-\frac{\pi}{4}\tau}\partial_\tau\,\frac{1}{a_{\mathrm{SR}}}H^{(2)}_{\nu_{\mathrm{SR}}}(-k(\tau+\Delta\tau_{\mathrm{SR}}))\sqrt{-\frac{\pi}{4}(\tau+\Delta\tau_{\mathrm{USR}})}\frac{1}{a_{\mathrm{USR}}}H^{(1)}_{\nu_{\mathrm{USR}}}(-k(\tau+\Delta\tau_{\mathrm{USR}}))\Bigg] \end{aligned} \tag{4.65}$$

where $\tau = \tau_{\mathrm{matching}}$.
The expression for beta looks as follows

$$\beta = -i(\phi^*\psi^{*\prime} - \phi^{*\prime}\psi^*) \tag{4.66}$$
$$= -i\left[\sqrt{-\frac{\pi}{4}(\tau+\Delta\tau_{\mathrm{SR}})}H^{(2)}_{\nu_{\mathrm{SR}}}(-k(\tau+\Delta\tau_{\mathrm{SR}}))\sqrt{-\frac{\pi}{4}(\tau+\Delta\tau_{\mathrm{USR}})}\partial_\tau H^{(2)}_{\nu_{\mathrm{USR}}}(-k(\tau+\Delta\tau_{\mathrm{USR}}))\right. \tag{4.67}$$
$$\begin{aligned} &+\frac{\frac{\pi}{4}(\Delta\tau_{\mathrm{USR}}-\Delta\tau_{\mathrm{SR}})}{\sqrt{(\tau+\Delta\tau_{\mathrm{SR}})(\tau+\Delta\tau_{\mathrm{USR}})}}H^{(2)}_{\nu_{\mathrm{SR}}}(-k(\tau+\Delta\tau_{\mathrm{SR}}))H^{(2)}_{\nu_{\mathrm{USR}}}(-k(\tau+\Delta\tau_{\mathrm{USR}}))\\ &\left.-\sqrt{-\frac{\pi}{4}(\tau+\Delta\tau_{\mathrm{SR}})}\partial_\tau\,H^{(2)}_{\nu_{\mathrm{SR}}}(-k(\tau+\Delta\tau_{\mathrm{SR}}))\sqrt{-\frac{\pi}{4}(\tau+\Delta\tau_{\mathrm{USR}})}H^{(2)}_{\nu_{\mathrm{USR}}}(-k(\tau+\Delta\tau_{\mathrm{USR}}))\right] \end{aligned}$$

We can now check if α and β obey the condition

$$|\alpha|^2 - |\beta|^2 = 1, \tag{4.68}$$

and they do. To first approximation, which gets better as $\frac{k}{aH}$ gets smaller, α and β look as follows

$$\alpha = \frac{-i}{2\pi a_{\mathrm{SR}} a_{\mathrm{USR}}} \Gamma(\nu_{\mathrm{SR}})\Gamma(\nu_{\mathrm{USR}})(\frac{k}{2})^{-\nu_{\mathrm{SR}}-\nu_{\mathrm{USR}}}(-(\tau+\Delta\tau_{\mathrm{SR}}))^{-\nu_{\mathrm{SR}}-\frac{1}{2}}(-(\tau+\Delta\tau_{\mathrm{USR}}))^{-\nu_{\mathrm{USR}}-\frac{1}{2}}$$
$$\frac{1}{2}[-\nu_{\mathrm{SR}}(\tau+\Delta\tau_{\mathrm{USR}}) + \nu_{\mathrm{USR}}(\tau+\Delta\tau_{\mathrm{SR}}) + \frac{1}{2}(\Delta\tau_{\mathrm{SR}} - \Delta\tau_{\mathrm{USR}})] \tag{4.69}$$

$$\beta = \frac{i}{2\pi a_{\mathrm{SR}} a_{\mathrm{USR}}} \Gamma(\nu_{\mathrm{SR}})\Gamma(\nu_{\mathrm{USR}})(\frac{-k}{2})^{-\nu_{\mathrm{SR}}-\nu_{\mathrm{USR}}}(\tau+\Delta\tau_{\mathrm{SR}})^{-\nu_{\mathrm{SR}}-\frac{1}{2}}(\tau+\Delta\tau_{\mathrm{USR}})^{-\nu_{\mathrm{USR}}-\frac{1}{2}}$$
$$\frac{1}{2}[\nu_{\mathrm{USR}}(\tau+\Delta\tau_{\mathrm{SR}}) - \nu_{\mathrm{SR}}(\tau+\Delta\tau_{\mathrm{USR}}) + \frac{1}{2}(\Delta\tau_{\mathrm{SR}} - \Delta\tau_{\mathrm{USR}})] \tag{4.70}$$

Better results are obtained when including the second order term

$$\alpha = \frac{-i}{2\pi a_{\mathrm{SR}} a_{\mathrm{USR}}} \Big[\Gamma(\nu_{\mathrm{SR}})\Gamma(\nu_{\mathrm{USR}})(\frac{k}{2})^{-\nu_{\mathrm{SR}}-\nu_{\mathrm{USR}}}(-(\tau+\Delta\tau_{\mathrm{SR}}))^{-\nu_{\mathrm{SR}}-\frac{1}{2}}(-(\tau+\Delta\tau_{\mathrm{USR}}))^{-\nu_{\mathrm{USR}}-\frac{1}{2}}$$
$$\times \Big(\frac{1}{2}[-\nu_{\mathrm{SR}}(\tau+\Delta\tau_{\mathrm{USR}}) + \nu_{\mathrm{USR}}(\tau+\Delta\tau_{\mathrm{SR}}) + \frac{1}{2}(\Delta\tau_{\mathrm{SR}} - \Delta\tau_{\mathrm{USR}})]$$
$$\times [1 - \frac{(-k\tau/2)^2}{-\nu_{\mathrm{SR}}+1} - \frac{(-k(\tau+\Delta\tau_{\mathrm{USR}})/2)^2}{-\nu_{\mathrm{USR}}+1} + \dots]$$
$$+\frac{-k(\tau+\Delta\tau_{\mathrm{SR}})(\tau+\Delta\tau_{\mathrm{USR}})}{2}[\frac{k(\tau+\Delta\tau_{\mathrm{SR}})/2}{-\nu_{\mathrm{SR}}+1} - \frac{k(\tau+\Delta\tau_{\mathrm{USR}})/2}{-\nu_{\mathrm{USR}}+1} + \dots]\Big)\Big] \tag{4.71}$$

$$\beta = \frac{i}{2\pi a_{\mathrm{SR}} a_{\mathrm{USR}}} \Big[\Gamma(\nu_{\mathrm{SR}})\Gamma(\nu_{\mathrm{USR}})(\frac{-k}{2})^{-\nu_{\mathrm{SR}}-\nu_{\mathrm{USR}}}(\tau+\Delta\tau_{\mathrm{SR}})^{-\nu_{\mathrm{SR}}-\frac{1}{2}}(\tau+\Delta\tau_{\mathrm{USR}})^{-\nu_{\mathrm{USR}}-\frac{1}{2}}$$
$$\times \Big(\frac{1}{2}[\nu_{\mathrm{USR}}(\tau+\Delta\tau_{\mathrm{SR}}) - \nu_{\mathrm{SR}}(\tau+\Delta\tau_{\mathrm{USR}}) + \frac{1}{2}(\Delta\tau_{\mathrm{SR}} - \Delta\tau_{\mathrm{USR}})]$$
$$\times [1 - \frac{(-k(\tau+\Delta\tau_{\mathrm{SR}})/2)^2}{-\nu_{\mathrm{SR}}+1} - \frac{(-k(\tau+\Delta\tau_{\mathrm{USR}})/2)^2}{-\nu_{\mathrm{USR}}+1} + \dots]$$
$$+\frac{-k(\tau+\Delta\tau_{\mathrm{SR}})(\tau+\Delta\tau_{\mathrm{USR}})}{2}[\frac{k(\tau+\Delta\tau_{\mathrm{SR}})/2}{-\nu_{\mathrm{SR}}+1} - \frac{k(\tau+\Delta\tau_{\mathrm{USR}})/2}{-\nu_{\mathrm{USR}}+1} + \dots]\Big)\Big], \tag{4.72}$$

and the full expressions can be found in the Appendix A.
In figure 4.5, it appears that the modes do not match, but approach the same value as time goes on when α and β are taken up to the sub-leading order term (equation 4.71) . If we take only the leading order into account (equation 4.69), we mismatch completely. The imaginary part of the modes is matched nicely at subleading (equation 4.71) order, but the real part mismatches, which causes the slight mismatch in figure 4.5. The expression including the subsub-leading (eq. A) order makes sure the real part is nicely matched. As the imaginary part is much larger than the real part, we find just a slight difference in the absolute value of the modes between using eq A and 4.71.

The absolute value of these modes decays. This happens, because while the Hankel functions grow with time, the scale factor grows faster, and the modes go with $\frac{1}{a}$. We can explain this as follows: The scale factor goes as $\frac{1}{a_{\mathrm{SR}}} \propto \tau^{\frac{1}{1-\epsilon_0}}$, and the leading order of the Hankel function goes$\propto \tau^{-\frac{3}{2}-\epsilon_0}$. This means that the full expression of the modes goes with $\frac{1}{a_{\mathrm{SR}}}\sqrt{\tau}\tau^{\nu_{\mathrm{SR}}} \propto \tau^{\epsilon_0^2+\mathcal{O}(\epsilon_0^3)}$. From this it is clear that there are no zeroth or first order terms in epsilon in this expression. Thus, the terms in which there is a zeroth or first order term in τ play an important role in the behaviour of the modes. This term is the sub-leading order in the Hankel function, which decays. The same is true during USR, but as ϵ_1 decays, the decay of the modes becomes slightly less than would be the case if we stayed in the SR regime.

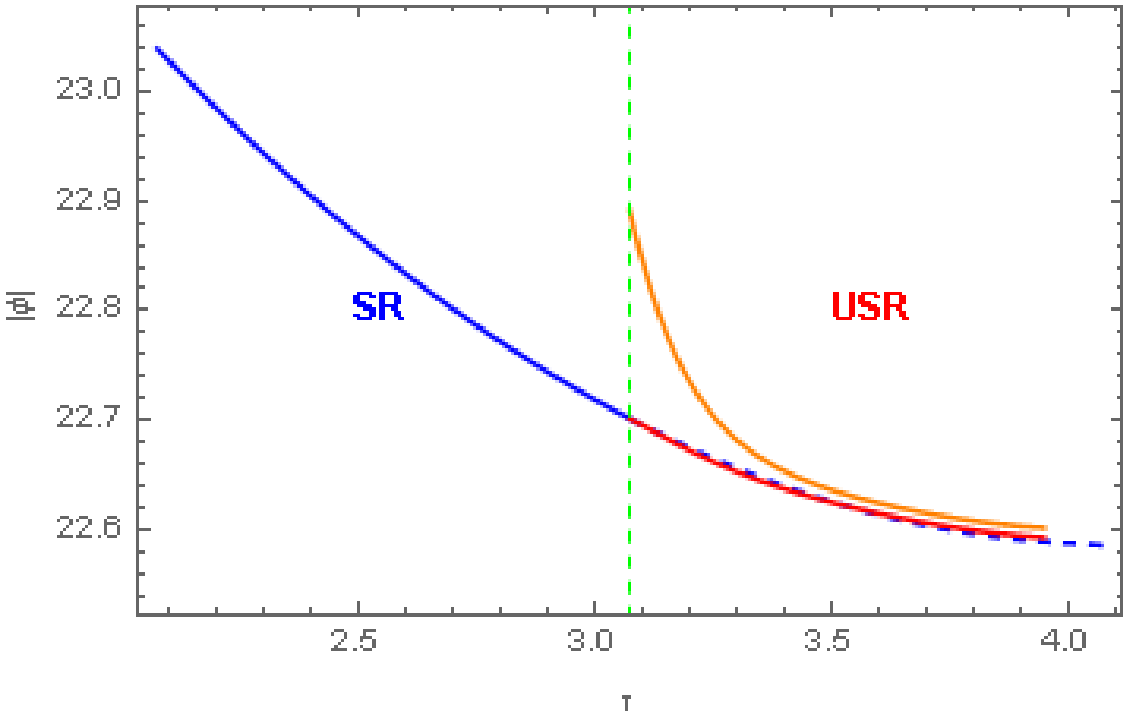

Figure 4.5: The absolute value of the matched modes with $\epsilon_0 = \frac{1}{200}$, $k = 0.1$, $a_0 = 1$ and $\mathcal{H}_0 = 1$. The blue line correspond to the mode in the slow-roll regime, the red to the modes in the ultra-slow-roll regime with the full expressions for α and β. The orange line corresponds to the approximate form of α and β as seen in eq. 4.71. The blue dotted line is the evolution that the modes would undergo if the SR approximation did not fail.

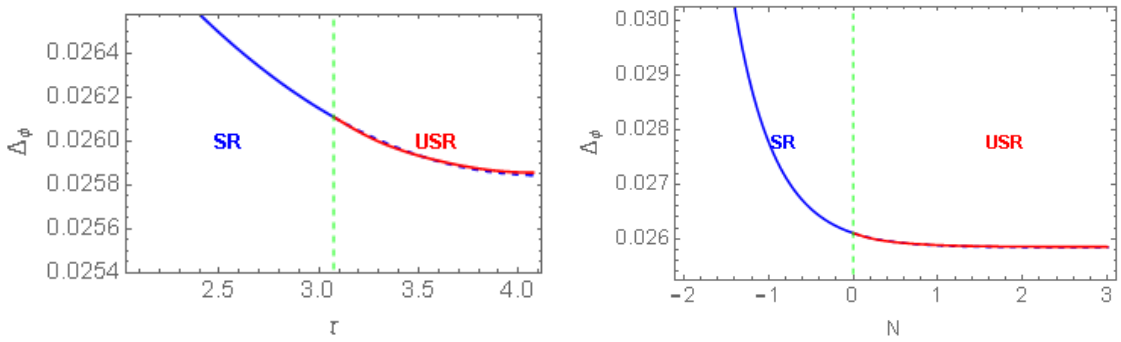

(a) The spectrum of the mode functions as a function of the conformal time τ.

(b) The spectrum of the mode functions as a function of the number of e-foldings N.

Figure 4.6: The spectrum of the mode functions as a function of two different time variables. The green line shows the time of matching, with the slow-roll regime on the left side, and the ultra-slow-roll on the right. Here we have used $\Delta\tau_{\rm SR}$ for the SR side and $\Delta\tau_{USR}$ for the USR side. The other constants that are used are $\mathcal{H}_0 = 1$, $\epsilon_0 = \frac{1}{200}$ and $k = 0.1$.

Now we should give some extra attention to the choice of $\Delta\tau_{\rm SR}$ and $\Delta\tau_{\rm USR}$, as this is quite subtle. We have determined these in such a way that the asymptotic behaviour of the scale factor and the Hubble parameter coincides with the asymptotic behaviour of the Hankel functions. We can view this as setting 'the time of the end of the universe'. However, if we do it this way, the values may slightly differ, and cause a jump in time at the time of matching. As we are interested in the late time behaviour, we could make the argument that this does not matter much, and we can just cut at the jump and glue the parts together, but this is a point of concern.

Alternatively, we can put $\Delta\tau$ the same on both sides. Now the question arises, which $\Delta\tau$ should we choose? We can argue for $\Delta\tau_{\rm USR}$, because USR is the regime where the asymptotic behaviour is going to play a role. On the other hand, we start in SR and match USR to this regime, so the SR part is the 'original'.

Note that results differ wildly for slightly different choice of $\Delta\tau_{\rm SR}$ and $\Delta\tau_{\rm USR}$. Our numerical value for $\Delta\tau_{\rm SR} = -4.07878$ and for $\Delta\tau_{\rm USR} = -4.07447$. As our solutions differ in $\mathcal{O}(\epsilon_1)$, this inequality of 0.1% is large enough to make a difference. In the first pictures of the power spectrum of the fluctuations in the inflaton field, we have taken $\Delta\tau_{\rm SR} = -\hat{\tau} - \frac{1}{a_0 H_0(1-\epsilon_0)} = -4.07878$ and $\Delta\tau_{\rm USR} = \lim_{a\to\infty} \tau(a) = -4.07447$.

When we take the same $\Delta\tau$ for both the SR and USR part, we see that one of the two goes to $\pm\infty$. When we take $\Delta\tau = \Delta\tau_{SR}$ in both cases, the modes in USR go to $-\infty$. This is because before we made sure the asymptotic behaviour of both the scale factor and the Hankel functions happened at the same τ, so they cancelled each other. Now the asymptote of the Hankel functions is at $\tau = \Delta\tau_{\rm SR}$, while the asymptote of the scale factor is still at $\Delta\tau_{\rm USR}$, which is later. The opposite happens with the hypothetical SR behaviour when we choose $\Delta\tau = \Delta\tau_{\rm USR}$. Here we pull the asymptote of the Hankel function to later times, which means that the asymptote in the scale factor makes the function blow up.

4.4 Spectra

To be able to compare the results with future observations, we should put it in a gauge-invariant and statistically measurable form. The spectrum of the curvature perturbation

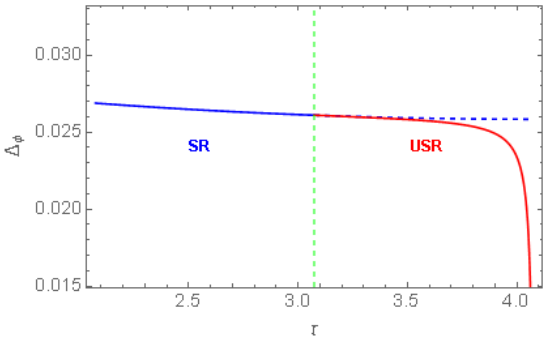

(a) The spectrum of the mode functions as a function of the conformal time τ.

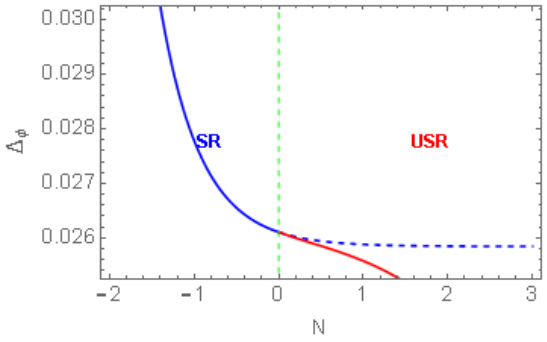

(b) The spectrum of the mode functions as a function of the number of e-foldings N.

Figure 4.7: The spectrum of the mode functions as a function of two different time variables. The green line shows the time of matching, with the slow-roll regime on the left side, and the ultra-slow-roll on the right. Here we have used $\Delta\tau_{\rm SR}$ for both sides. The other constants that are used are $\mathcal{H}_0 = 1$, $\epsilon_0 = \frac{1}{200}$ and $k = 0.1$.

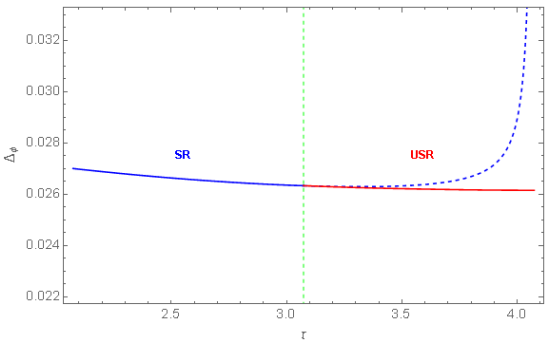

(a) The spectrum of the mode functions as a function of the conformal time τ.

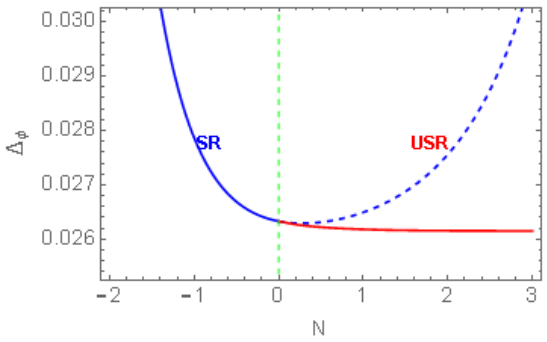

(b) The spectrum of the mode functions as a function of the number of e-foldings N.

Figure 4.8: The spectrum of the mode functions as a function of two different time variables. The green line shows the time of matching, with the slow-roll regime on the left side, and the ultra-slow-roll on the right. Here we have used $\Delta\tau_{USR}$ for both sides. The other constants that are used are $\mathcal{H}_0 = 1$, $\epsilon_0 = \frac{1}{200}$ and $k = 0.1$.

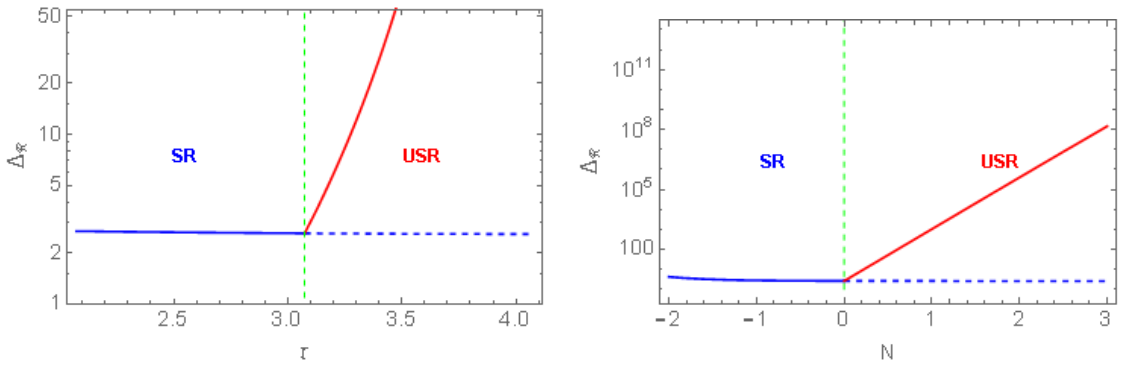

(a) The spectrum of the mode functions as a function of the conformal time τ.

(b) The spectrum of the mode functions as a function of the number of e-foldings N.

Figure 4.9: The curvature spectrum of the mode functions as a function of two different time variables. The green line shows the time of matching, with the slow-roll regime on the left side, and the ultra-slow-roll on the right. Here we have used $\Delta\tau_{\rm SR}$ for the SR side and $\Delta\tau_{USR}$ for the USR side.

is, as explained in the previous chapter, given by

$$\Delta^2_{\mathcal{R}} = \frac{1}{2\epsilon_1}\frac{k^3}{2\pi^2}|\delta\phi(\vec{k},\tau)|^2. \tag{4.73}$$

We have plotted the curvature power spectrum for our matched modes, as a function of different time parameters. We have again plotted the spectrum for $\Delta\tau_{\rm SR}$ on the SR side and $\Delta\tau_{\rm USR}$ on the USR side (see figure 4.9), $\Delta\tau_{\rm SR}$ on both sides (see figure 4.10) and $\Delta\tau_{\rm USR}$ on both sides (see figure 4.11). Here the difference between figure 4.9 and 4.10 can not been seen anymore, because $\frac{1}{\epsilon_1}$ also grows very fast. The difference between figure 4.9 and 4.11 is clearly visible. This, however, does not give rise to different conclusions, as the difference is mostly in the part that is only hypothetical. In Appendix B, we also show linear plots of the curvature power spectrum.

This spectrum is not the true spectrum, which would not be larger then one, because of our choice $H_0 = 1$. To recover the true spectrum, the Planck mass should be reintroduced or it could be put to one, which together with the COBE normalization implies a certain value for H_0. Then the spectrum should obey the COBE constraint [26].

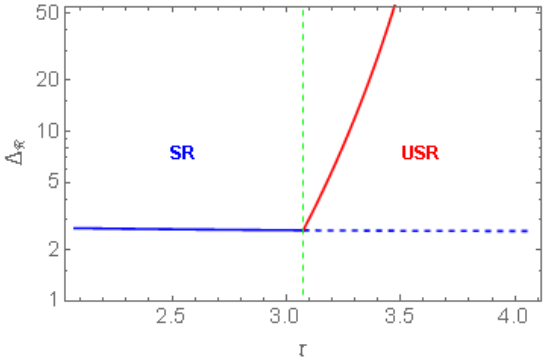

(a) The spectrum of the mode functions as a function of the conformal time τ.

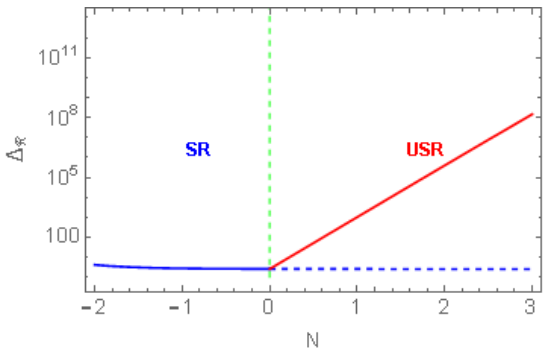

(b) The spectrum of the mode functions as a function of the number of e-foldings N.

Figure 4.10: The curvature spectrum of the mode functions as a function of two different time variables. The green line shows the time of matching, with the slow-roll regime on the left side, and the ultra-slow-roll on the right. Here we have used $\Delta\tau_{SR}$ for both sides.

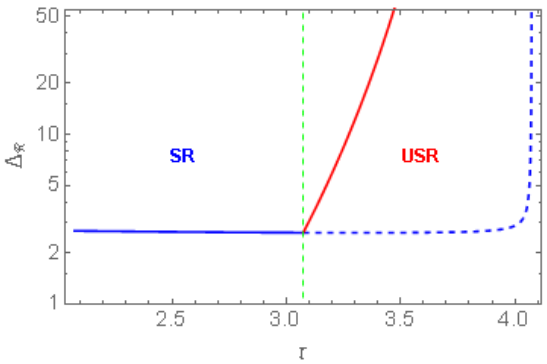

(a) The spectrum of the mode functions as a function of the conformal time τ.

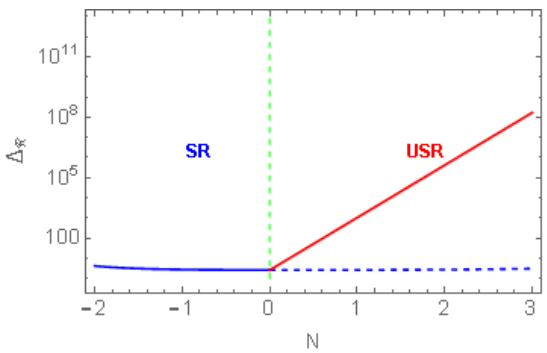

(b) The spectrum of the mode functions as a function of the number of e-foldings N.

Figure 4.11: The curvature spectrum of the mode functions as a function of two different time variables. The green line shows the time of matching, with the slow-roll regime on the left side, and the ultra-slow-roll on the right. Here we have used $\Delta\tau_{USR}$ for both sides.

4.5 The Bigger Picture and Discussion

4.5.1 Comparison with earlier research

In a recent paper, Cheng et al. studied super-horizon perturbation during a period of SR, followed by USR, followed by SR [27]. They found that if they used $\epsilon_2 < 0$, which is what we have used, the power spectrum was amplified. This is in agreement with our results. Although, they did not match the background or take corrections of $\mathcal{O}(\epsilon_1)$ into account.

In the appendix of a paper by Byrnes et al. [28], a matching is performed between SR and USR and back to SR. Here they also do not take corrections of order ϵ_1 into account in their derivation of ν_{USR} and therefore in their derivation of the modes. They do find an exponentially growing spectrum during USR, as we did.

To really compare our results to theirs, we should first perform the matching from USR back to SR. For the time being, it seems that we do not find wildly different results from others.

4.5.2 Discussion of the choice of $\Delta\tau$

A different choice of $\Delta\tau$ can considerably change the results of the power spectrum of the modes, and can slightly change the power spectrum of the curvature perturbations. Here future research can probably make much clearer which choices must be made and why. A possibility is to take $z = \frac{k}{aH(1-\epsilon_0)}$ in stead of $z = -k(\tau + \Delta\tau)$ in the Hankel functions $H_\nu^{(1),(2)}(z)$ in future research, as in this way the problem can be avoided. Let's analyse the problem a bit closer: To prevent the jump in time, we need

$$-k(\tau + \Delta\tau_{\text{SR}}) = -k(\tau + \Delta\tau_{\text{USR}}) \tag{4.74}$$

to be true. And while we know that

$$\frac{k}{a_{\text{SR}}H_{\text{SR}}(1-\epsilon_0)} = \frac{k}{a_{\text{SR}}H_{\text{USR}}(1-\epsilon_1)}, \quad \text{at the time of matching,} \tag{4.75}$$

if

$$-k(\tau + \Delta\tau_{\text{SR}}) = \frac{k}{a_{\text{SR}}H_{\text{SR}}(1-\epsilon_0)} \tag{4.76}$$

and

$$-k(\tau + \Delta\tau_{\text{USR}}) = \frac{k}{a_{\text{USR}}H_{\text{USR}}(1-\epsilon_1)}, \tag{4.77}$$

the following should also be true everywhere,

$$a_{\text{SR}}H_{\text{SR}}(1-\epsilon_0) = a_{\text{USR}}H_{\text{USR}}(1-\epsilon_1). \tag{4.78}$$

This is not the case in this thesis, which may be the cause of our problem. If we do take these definitions, we can in principle find an alternative $\Delta\tau_{\text{USR}}$ by taking

$$\Delta\tau_{\text{USR}} = \frac{-1}{a_{\text{USR}}H_{\text{USR}}(1-\epsilon_1)} - \tau \tag{4.79}$$

For $\tau \to \infty$ this goes to a constant, which is what we have used for $\Delta\tau_{\text{USR}}$. This means that we effectively created a jump in τ at the time of matching, but as we are only looking at late times, this is probably fine. We analytically extend the solution back to the time of matching.

Chapter 5

Conclusion and Outlook

Curvature perturbations rapidly grow during a period of USR, where the first SR parameter rapidly decreases. This increases the probability of primordial black holes to form, as they are created by the collapsing of overdense regions. We matched the SR regime to the USR regime, where we included a matching of the background. The background does not show large changes, as the changes are of order ϵ. Most of the growth of the curvature perturbation power spectrum can be attributed to the decline of ϵ_1 in the definition of the curvature perturbation power spectrum, and just a small part is contributed by the growth of the spectrum of the inflaton perturbations.

To do this matching procedure, we found an exact expression for the conformal time τ, expressed in the number of e-foldings N since the matching, with the use of hypergeometric functions

$$\tau + \Delta\tau = \frac{1}{2a_0 H_0 \sqrt{\frac{\epsilon_0}{3}}} e^{2N} \, {}_2F_1\left(\frac{1}{2}, \frac{1}{3}; \frac{4}{3}; -(3/\epsilon_0 - 1)e^{6N}\right). \tag{5.1}$$

This is a new result, and can be used to rewrite expressions in terms of the other time variable during USR inflation.

We also found expressions for the Bogoliubov coefficients (equations A.1 and A.2). We suspected that it would be enough to only take the leading order terms, but to ensure a smooth matching and the correct behaviour at later times, we should also take the other terms into account. This brings into question the practise of using only the leading order contribution, which is common in related research.

As proposed in the last section, the dependence in the Hankel functions can be taken more precisely to be $z = \frac{k}{aH(1-\epsilon_0)}$. This will ensure that there is no discontinuity in time. If this is done, it needs to be considered that after a period of SR inflation will probably follow a USR period. So future research should match the USR period to another period of SR. This can be done in much the same way, and will give the full evolution of the modes. This will also mean that the primordial spectrum after inflation can be calculated, from which it is possible to compare our results with future observations.

Acknowledgements

I would like to thank dr. Tomislav Prokopec, for giving me this opportunity and making time in his busy schedule to help me.

I would like to thank the spell checker in Latex, for correcting me every time I type 'inlfation'.

I would like to thank the students in the 'Ivoren Toren' for running down the stairs with me.

I would like to thank A–Eskwadraat for all the free coffee and tea.

I would like to thank my family and friends for supporting me all this time.

Appendix A

Full expressions for alpha and beta

Here are the expressions for the Bogoliubov coefficients in their full glory,

$$
\begin{aligned}
\alpha =& \frac{-i}{4\pi a_{\mathrm{SR}} a_{\mathrm{USR}}} \Bigg[e^{\pi i(\nu_{SR}-\nu_{USR})}\Gamma(-\nu_{SR})\Gamma(-\nu_{USR})(\frac{k}{2})^{\nu_{SR}+\nu_{USR}}(-(\tau+\Delta\tau_{SR}))^{\nu_{SR}-\frac{1}{2}} \\
&\times(-(\tau+\Delta\tau_{USR}))^{\nu_{USR}-\frac{1}{2}}\Bigg(\\
&\quad [\nu_{SR}(\tau+\Delta\tau_{USR})-\nu_{USR}(\tau+\Delta\tau_{SR})-\frac{1}{2}(\Delta\tau_{SR}-\Delta\tau_{USR})] \\
&\quad \times[1-\frac{(-k(\tau+\Delta\tau_{SR})/2)^2}{\nu_{SR}+1}-\frac{(-k(\tau+\Delta\tau_{USR})/2)^2}{\nu_{USR}+1}+\dots] \\
&\quad -k(\tau+\Delta\tau_{SR})(\tau+\Delta\tau_{USR})[\frac{k(\tau+\Delta\tau_{SR})/2}{\nu_{SR}+1}-\frac{k(\tau+\Delta\tau_{USR})/2}{\nu_{USR}+1}+\dots]\Bigg) \\
&+ e^{\pi i\nu_{SR}}\Gamma(-\nu_{SR})\Gamma(\nu_{USR})(\frac{k}{2})^{\nu_{SR}-\nu_{USR}}(-(\tau+\Delta\tau_{SR}))^{\nu_{SR}-\frac{1}{2}}(-(\tau+\Delta\tau_{USR}))^{-\nu_{USR}-\frac{1}{2}}\Bigg(\\
&\quad [\nu_{SR}(\tau+\Delta\tau_{USR})+\nu_{USR}(\tau+\Delta\tau_{SR})-\frac{1}{2}(\Delta\tau_{SR}-\Delta\tau_{USR})] \\
&\quad \times[1-\frac{(-k(\tau+\Delta\tau_{SR})/2)^2}{\nu_{SR}+1}-\frac{(-k(\tau+\Delta\tau_{USR})/2)^2}{-\nu_{USR}+1}+\dots] \\
&\quad -k(\tau+\Delta\tau_{SR})(\tau+\Delta\tau_{USR})[\frac{k(\tau+\Delta\tau_{SR})/2}{\nu_{SR}+1}-\frac{k(\tau+\Delta\tau_{USR})/2}{-\nu_{USR}+1}+\dots]\Bigg) \\
&+ e^{-\pi i\nu_{USR}}\Gamma(\nu_{SR})\Gamma(-\nu_{USR})(\frac{k}{2})^{-\nu_{SR}+\nu_{USR}}(-(\tau+\Delta\tau_{SR}))^{-\nu_{SR}-\frac{1}{2}}(\tau+\Delta\tau_{USR})^{\nu_{USR}-\frac{1}{2}}\Bigg(\\
&\quad [-\nu_{SR}(\tau+\Delta\tau_{USR})-\nu_{USR}(\tau+\Delta\tau_{SR})-\frac{1}{2}(\Delta\tau_{SR}-\Delta\tau_{USR})] \\
&\quad \times[1-\frac{(-k(\tau+\Delta\tau_{SR})/2)^2}{-\nu_{SR}+1}-\frac{(-k(\tau+\Delta\tau_{USR})/2)^2}{\nu_{USR}+1}+\dots] \\
&\quad -k(\tau+\Delta\tau_{SR})(\tau+\Delta\tau_{USR})[\frac{k(\tau+\Delta\tau_{SR})/2}{-\nu_{SR}+1}-\frac{k(\tau+\Delta\tau_{USR})/2}{\nu_{USR}+1}+\dots]\Bigg) \\
&+ \Gamma(\nu_{SR})\Gamma(\nu_{USR})(\frac{k}{2})^{-\nu_{SR}-\nu_{USR}}(-(\tau+\Delta\tau_{SR}))^{-\nu_{SR}-\frac{1}{2}}(-(\tau+\Delta\tau_{USR}))^{-\nu_{USR}-\frac{1}{2}}\Bigg(\\
&\quad [-\nu_{SR}(\tau+\Delta\tau_{USR})+\nu_{USR}(\tau+\Delta\tau_{SR})-\frac{1}{2}(\Delta\tau_{SR}-\Delta\tau_{USR})] \\
&\quad \times[1-\frac{(-k\tau/2)^2}{-\nu_{SR}+1}-\frac{(-k(\tau+\Delta\tau_{USR})/2)^2}{-\nu_{USR}+1}+\dots] \\
&\quad -k(\tau+\Delta\tau_{SR})(\tau+\Delta\tau_{USR})[\frac{k(\tau+\Delta\tau_{SR})/2}{-\nu_{SR}+1}-\frac{k(\tau+\Delta\tau_{USR})/2}{-\nu_{USR}+1}+\dots]\Bigg)\Bigg],
\end{aligned}
\tag{A.1}
$$

$$
\begin{aligned}
\beta =& \frac{i}{4\pi a_{\rm SR} a_{\rm USR}} \Bigg[e^{\pi i(\nu_{SR}+\nu_{USR})}\Gamma(-\nu_{SR})\Gamma(-\nu_{USR})(\frac{-k}{2})^{\nu_{SR}+\nu_{USR}}(\tau+\Delta\tau_{SR})^{\nu_{SR}-\frac{1}{2}} \\
&\times(\tau+\Delta\tau_{USR})^{\nu_{USR}-\frac{1}{2}} \Bigg(\\
&\quad [-\nu_{USR}(\tau+\Delta\tau_{SR})+\nu_{SR}(\tau+\Delta\tau_{USR})-\frac{1}{2}(\Delta\tau_{SR}-\Delta\tau_{USR})] \\
&\quad \times [1-\frac{(-k(\tau+\Delta\tau_{SR})/2)^2}{\nu_{SR}+1}-\frac{(-k(\tau+\Delta\tau_{USR})/2)^2}{\nu_{USR}+1}+\dots] \\
&\quad -k(\tau+\Delta\tau_{SR})(\tau+\Delta\tau_{USR})[\frac{k(\tau+\Delta\tau_{SR})/2}{\nu_{SR}+1}-\frac{k(\tau+\Delta\tau_{USR})/2}{\nu_{USR}+1}+\dots]\Bigg) \\
&+ e^{\pi i\nu_{SR}}\Gamma(-\nu_{SR})\Gamma(\nu_{USR})(\frac{-k}{2})^{\nu_{SR}-\nu_{USR}}(\tau+\Delta\tau_{SR})^{\nu_{SR}-\frac{1}{2}}(\tau+\Delta\tau_{USR})^{-\nu_{USR}-\frac{1}{2}} \Bigg(\\
&\quad [\nu_{USR}(\tau+\Delta\tau_{SR})+\nu_{SR}(\tau+\Delta\tau_{USR})-\frac{1}{2}(\Delta\tau_{SR}-\Delta\tau_{USR})] \\
&\quad \times [1-\frac{(-k(\tau+\Delta\tau_{SR})/2)^2}{\nu_{SR}+1}-\frac{(-k(\tau+\Delta\tau_{USR})/2)^2}{-\nu_{USR}+1}+\dots] \\
&\quad -k(\tau+\Delta\tau_{SR})(\tau+\Delta\tau_{USR})[\frac{k(\tau+\Delta\tau_{SR})/2}{\nu_{SR}+1}-\frac{k(\tau+\Delta\tau_{USR})/2}{-\nu_{USR}+1}+\dots]\Bigg) \\
&+ e^{\pi i\nu_{USR}}\Gamma(\nu_{SR})\Gamma(-\nu_{USR})(\frac{-k}{2})^{-\nu_{SR}+\nu_{USR}}(\tau+\Delta\tau_{SR})^{-\nu_{SR}-\frac{1}{2}}(\tau+\Delta\tau_{USR})^{\nu_{USR}-\frac{1}{2}} \Bigg(\\
&\quad [-\nu_{USR}(\tau+\Delta\tau_{SR})-\nu_{SR}(\tau+\Delta\tau_{USR})-\frac{1}{2}(\Delta\tau_{SR}-\Delta\tau_{USR})] \\
&\quad \times [1-\frac{(-k(\tau+\Delta\tau_{SR})/2)^2}{-\nu_{SR}+1}-\frac{(-k(\tau+\Delta\tau_{USR})/2)^2}{\nu_{USR}+1}+\dots] \\
&\quad -k(\tau+\Delta\tau_{SR})(\tau+\Delta\tau_{USR})[\frac{k(\tau+\Delta\tau_{SR})/2}{-\nu_{SR}+1}-\frac{k(\tau+\Delta\tau_{USR})/2}{\nu_{USR}+1}+\dots]\Bigg) \\
&+ \Gamma(\nu_{SR})\Gamma(\nu_{USR})(\frac{-k}{2})^{-\nu_{SR}-\nu_{USR}}(\tau+\Delta\tau_{SR})^{-\nu_{SR}-\frac{1}{2}}(\tau+\Delta\tau_{USR})^{-\nu_{USR}-\frac{1}{2}} \Bigg(\\
&\quad [\nu_{USR}(\tau+\Delta\tau_{SR})-\nu_{SR}(\tau+\Delta\tau_{USR})-\frac{1}{2}(\Delta\tau_{SR}-\Delta\tau_{USR})] \\
&\quad \times [1-\frac{(-k(\tau+\Delta\tau_{SR})/2)^2}{-\nu_{SR}+1}-\frac{(-k(\tau+\Delta\tau_{USR})/2)^2}{-\nu_{USR}+1}+\dots] \\
&\quad -k(\tau+\Delta\tau_{SR})(\tau+\Delta\tau_{USR})[\frac{k(\tau+\Delta\tau_{SR})/2}{-\nu_{SR}+1}-\frac{k(\tau+\Delta\tau_{USR})/2}{-\nu_{USR}+1}+\dots]\Bigg)\Bigg] .
\end{aligned}
\tag{A.2}
$$

Appendix B

Linear plots of the curvature spectrum

In the main text we have shown the logaritmic plots of the curvature power spectrum, here we put the linear plots.

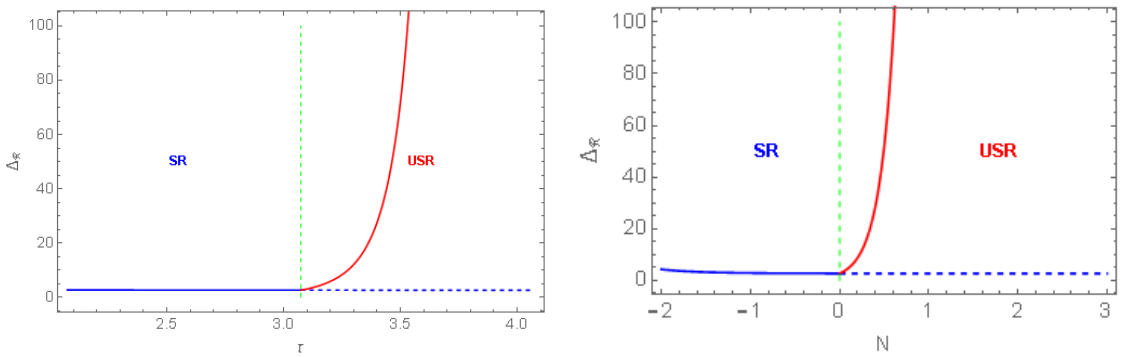

(a) The spectrum of the mode functions as a function of the conformal time τ.

(b) The spectrum of the mode functions as a function of the number of e-foldings N.

Figure B.1: The curvature spectrum of the mode functions as a function of two different time variables. The green line shows the time of matching, with the slow-roll regime on the left side, and the ultra-slow-roll on the right.

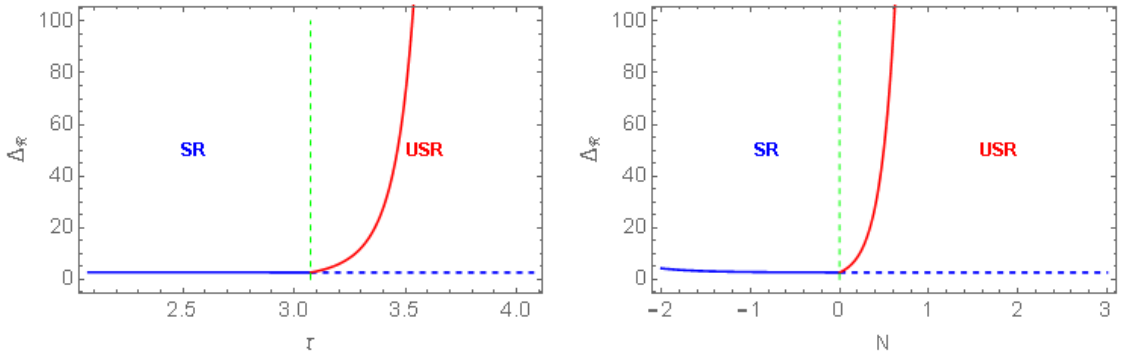

(a) The spectrum of the mode functions as a function of the conformal time τ.

(b) The spectrum of the mode functions as a function of the number of e-foldings N.

Figure B.2: The curvature spectrum of the mode functions as a function of two different time variables. The green line shows the time of matching, with the slow-roll regime on the left side, and the ultra-slow-roll on the right.

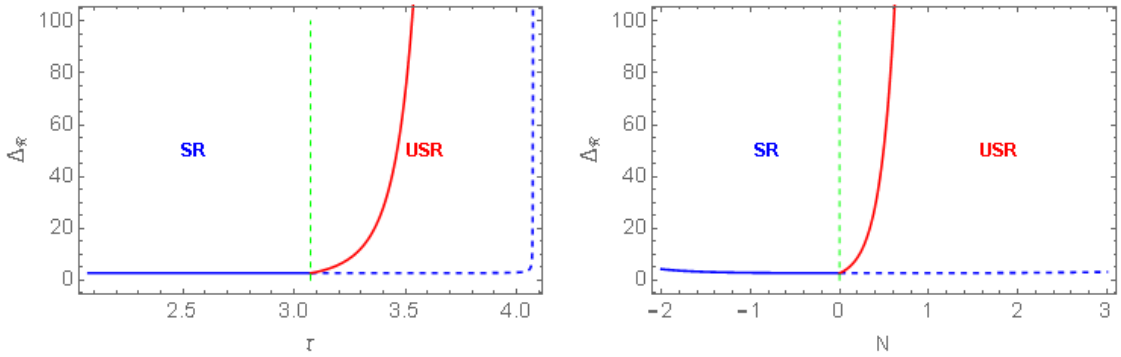

(a) The spectrum of the mode functions as a function of the conformal time τ.

(b) The spectrum of the mode functions as a function of the number of e-foldings N.

Figure B.3: The curvature spectrum of the mode functions as a function of two different time variables. The green line shows the time of matching, with the slow-roll regime on the left side, and the ultra-slow-roll on the right.

Bibliography

[1] Gianfranco Bertone and Dan Hooper. History of dark matter. *Reviews of Modern Physics*, 90(4):045002, Oct 2018.

[2] J. G. de Swart, G. Bertone, and J. van Dongen. How dark matter came to matter. *Nature Astronomy*, 1:0059, Mar 2017.

[3] William Thomson, Baron Kelvin. *Baltimore Lectures on Molecular Dynamics and the Wave Theory of Light*. Cambridge Library Collection - Physical Sciences. Cambridge University Press, 2010.

[4] F. Zwicky. Die Rotverschiebung von extragalaktischen Nebeln. *Helv. Phys. Acta*, 6:110–127, 1933. [Gen. Rel. Grav.41,207(2009)].

[5] Sinclair Smith. The Mass of the Virgo Cluster. , 83:23, Jan 1936.

[6] E. Holmberg. A Study of Double and Multiple Galaxies Together with Inquiries into some General Metagalactic Problems. *Annals of the Observatory of Lund*, 6:1–173, 1937.

[7] E. Hubble and M. L. Humason. The Velocity-Distance Relation among Extra-Galactic Nebulae. , 74:43, July 1931.

[8] F. Zwicky. On the Masses of Nebulae and of Clusters of Nebulae. *Astrophys. J.*, 86:217–246, 1937.

[9] D. H. Rogstad and G. S. Shostak. Gross Properties of Five Scd Galaxies as Determined from 21-CENTIMETER Observations. , 176:315, Sep 1972.

[10] J. P. Ostriker, P. J. E. Peebles, and A. Yahil. The size and mass of galaxies, and the mass of the universe. , 193:L1–L4, October 1974.

[11] J. Einasto, A. Kaasik, and E. Saar. Dynamic evidence on massive coronas of galaxies. , 250:309–310, July 1974.

[12] Giorgio Arcadi, Maíra Dutra, Pradipta Ghosh, Manfred Lindner, Yann Mambrini, Mathias Pierre, Stefano Profumo, and Farinaldo S. Queiroz. The waning of the WIMP? A review of models, searches, and constraints. *European Physical Journal C*, 78(3):203, Mar 2018.

[13] Marc Schumann. Direct Detection of WIMP Dark Matter: Concepts and Status. *arXiv e-prints*, page arXiv:1903.03026, Mar 2019.

[14] Y. B. Zel'dovich and I. D. Novikov. The Hypothesis of Cores Retarded during Expansion and the Hot Cosmological Model. , 10:602, February 1967.

[15] S. Hawking. Gravitationally collapsed objects of very low mass. , 152:75, 1971.

[16] Juan García-Bellido, Andrei Linde, and David Wands. Density perturbations and black hole formation in hybrid inflation. , 54(10):6040–6058, Nov 1996.

[17] Juan García-Bellido. Massive Primordial Black Holes as Dark Matter and their detection with Gravitational Waves. In *Journal of Physics Conference Series*, volume 840 of *Journal of Physics Conference Series*, page 012032, May 2017.

[18] Daniel Baumann. TASI Lectures on Inflation. *arXiv e-prints*, page arXiv:0907.5424, Jul 2009.

[19] S. Weinberg. *Cosmology*. Cosmology. OUP Oxford, 2008.

[20] Andrew R. Liddle, Paul Parsons, and John D. Barrow. Formalizing the slow-roll approximation in inflation. , 50(12):7222–7232, Dec 1994.

[21] Konstantinos Dimopoulos. Ultra slow-roll inflation demystified. *Physics Letters B*, 775:262–265, Dec 2017.

[22] Diego Cruces, Cristiano Germani, and Tomislav Prokopec. Failure of the stochastic approach to inflation beyond slow-roll. *Journal of Cosmology and Astro-Particle Physics*, 2019(3):048, Mar 2019.

[23] A.R. Liddle and D.H. Lyth. *Cosmological Inflation and Large-Scale Structure*. Cosmological Inflation and Large-scale Structure. Cambridge University Press, 2000.

[24] Viatcheslav F. Mukhanov, H. A. Feldman, and Robert H. Brandenberger. Theory of cosmological perturbations. Part 1. Classical perturbations. Part 2. Quantum theory of perturbations. Part 3. Extensions. *Phys. Rept.*, 215:203–333, 1992.

[25] I.S. Gradshteyn and I.M. Ryzhik. *Table of Integrals, Series, and Products*. Jul 1980.

[26] Emory F. Bunn, Andrew R. Liddle, and Martin White. Four-year COBE normalization of inflationary cosmologies. , 54(10):R5917–R5921, Nov 1996.

[27] Shu-Lin Cheng, Wolung Lee, and Kin-Wang Ng. Superhorizon curvature perturbation in ultraslow-roll inflation. , 99(6):063524, Mar 2019.

[28] Christian T. Byrnes, Philippa S. Cole, and Subodh P. Patil. Steepest growth of the power spectrum and primordial black holes. , 2019(6):028, Jun 2019.